# N-3 POLYUNSATURATED FATTY ACIDS REDUCE TH17 DIFFERENTIATION BY DECREASING RESPONSIVENESS TO INTERLEUKIN-6 IN MICE

A Thesis

by

MARILYN JEAN ALLEN

Submitted to the Office of Graduate and Professional Studies of
Texas A&M University
in partial fulfillment of the requirements for the degree of

MASTER OF SCIENCE

| | |
|---|---|
| Chair of Committee, | Robert S. Chapkin |
| Committee Members, | David N. McMurray |
| | Jane Welsh |
| Head of Department, | Jimmy Keeton |

August 2014

Major Subject: Nutrition

ABSTRACT

$CD4^+$ effector T cell subsets (e.g., Th1, Th17) are implicated in autoimmune and inflammatory disorders such as multiple sclerosis, psoriasis and rheumatoid arthritis. For optimal activation, IL-6 induces Th17 polarization and signals through the membrane-bound signal transducer, gp130. Previously, we have demonstrated that n-3 polyunsaturated fatty acids (PUFA), when supplied in the diet or in *fat-1* transgenic mice which generate n-3 PUFA de novo, suppress $CD4^+$ T cell activation and differentiation into pathogenic Th17 cells. Here we report that n-3 PUFA alter the response of $CD4^+$ T cells to IL-6 in a lipid raft membrane-dependent fashion. Naïve splenic $CD4^+$ T cells from *fat-1* mice exhibited significantly lower surface expression of the IL-6 receptor (IL-6R). This membrane bound receptor is known to be shed upon cellular activation in response to antigen; however, the release of soluble IL-6R after treatment with anti-CD3 and anti-CD28 was not changed in *fat-1* mice suggesting that the decrease in surface expression is not due to ectodomain release. We observed a significant decrease in the association of gp130 with lipid rafts in activated *fat-1* $CD4^+$ T cells and a 35% reduction in gp130 homodimerization, an obligate requirement for downstream signaling. The phosphorylation of STAT3, a downstream target of IL-6-dependent signaling, was also decreased in response to exogenous IL-6 in *fat-1* $CD4^+$ T cells. Our results suggest that n-3 PUFA suppress Th17 cell differentiation, in part, by reducing membrane raft-dependent responsiveness to IL-6, an essential polarizing cytokine.

ACKNOWLEDGEMENTS

I couldn't have finished this project without the help of my lab. Thank you to Tim Hou, Dr. Yang-Yi Fan, Dr. Laurie Davidson and Evelyn Callaway for training and encouraging me over the last two years. Thank you to my mentor, Dr. Robert Chapkin, for your patience and guidance during this experience. A big thanks also to my other committee members, Dr. David McMurray and Dr. Jane Welsh for helping me with project development and writing. My family has also been a great help; I am very grateful to everyone especially Angie for her support.

TABLE OF CONTENTS

Page

LIST OF FIGURES

Page

# INTRODUCTION

## *Role of CD4$^+$ T cells in inflammatory diseases*

Chronic diseases such as cancer, cardiovascular disease and stroke are currently the leading causes of death in the United States. Many of these diseases are linked to inflammation including arthritis, multiple sclerosis (1), obesity, diabetes (2) and cancer (3) as well as the normal process of aging (4). Effector CD4$^+$ T cells, especially Th1 and Th17 cells play an important role in both driving and resolving inflammatory processes. While effector T cells act to eradicate invading pathogens, another subset of CD4$^+$ T cells, the Tregs function to suppress T cell activation as well as prevent reactivity against host tissue and subsequent autoimmune disease (5). The main functions of CD4$^+$ T cells include cytokine production and B cell activation as well as tolerance to self-antigens (6). CD4$^+$ T cells themselves are incapable of responding to a free antigen; instead they require the help of an antigen presenting cell (APC) which internalizes the antigen and processes it for presentation to the CD4$^+$T cell via the major histocompatibility complex (MHC). The MHC, in turn, interacts with the T cell receptor (TCR) forming an immunological synapse. Th17 cells differentiate from naïve CD4$^+$ T cells under the influence of interleukin-6 (IL-6) and TGF-β (5,7) which activate STAT3. Phosphorylation of STAT3 leads to translocation to the nucleus and subsequent activation of ROR-γt, the master regulator of Th17 transcription. IL-23R is upregulated on the cell surface and contributes to the maintenance and expansion of mature Th17 cells (8). Th17 cells function primarily to stimulate a neutrophil response in the presence of extracellular bacteria and are characterized by the release of IL-17A, IL-17F, IL-21

and IL-22 (3).

Th17 cells play an important role in the immune response, especially in the clearance of extracellular bacteria and viruses (9). This occurs through the action of cytokines. Specifically, IL-17 is involved in stimulating granulopoiesis and neutrophil chemotaxis (7,10) and IL-22 works by stimulating epithelial cell proliferation to enhance epithelial barrier function (11). Additionally, IL-22 induces the production of REG proteins (12) and protective mucus (13). Finally, IL-22 works with IL-17 to induce the production of antimicrobial proteins (14). However, if this response is not resolved after the pathogen is cleared, chronic inflammation and tissue damage ensue. Specifically, chronic Th17-mediated inflammation in the colon has been linked to the onset of inflammatory bowel diseases (IBD) and to colitis-associated cancer (CAC) (15). A chronic pronounced elevation in the IL-6/gp130/STAT3 signaling axis is considered a risk factor for colorectal cancer due in part to stimulation of epithelial cell proliferation (16). Further investigation suggests that dysregulation of IL-6 signaling leads to gastric cancer through a STAT3 related mechanism (17), and its inhibition can reduce tumor development in colitis-induced cancer model (16) and multiple sclerosis (18). Additionally, IL-6 present in serum prevents the polarization of T regulatory cells (18,19) while a deficiency in IL-6 leads to defective T cell recruitment after tissue injury (20).

***Effect of n-3 PUFA on inflammation***

Many dietary components affect the inflammatory process including n-3 polyunsaturated fatty acids (PUFA). n-3 PUFA contain a double bond at the third carbon from the methyl end of the carbon chain. The human body cannot synthesize n-3 PUFA due to the lack of long chain desaturases that work beyond the Δ9 position (21). Eicosapentaenoic acid (EPA) (20:5n-3) and docosahexaenoic acid (DHA) (22:6n-3) are two examples of bioactive fatty acids which exhibit anti-inflammatory affects (22,23). n-3 PUFA are known to have many health benefits including a reduction of blood triglycerides (24,25) blood pressure (26) and platelet aggregation (27). Alpha-linolenic acid is found in leafy green vegetables, walnuts and rapeseed and flaxseed oils while EPA and DHA are found in marine sources such as salmon, shrimp, herring and sardines (28). The typical American diet contains 1.1-1.6 g/d n-3 PUFA including 110-230 mg/d EPA + DHA. Unfortunately, this is far below the suggested recommendation of 500 mg/d EPA + DHA which could be accomplished by two fish meals per week (28,29). Previously, intake of EPA, DPA and DHA (long chain n-3 PUFA or n-3 LCFA) was estimated based upon food disappearance data in 42 countries. The United States ranked in the middle with 0.103% of energy coming from n-3 LCFA or 230 mg/d on a 2000 kcal diet. Among the highest intakes were Iceland (0.435% of energy or 960 mg/d) and Japan (0.374% of energy or 831 mg/d). Bulgaria (0.023% of energy or 51 mg/d) and Romania (0.041% of energy or 91 mg/d) consumed the least n-3 LCFA (29). Epidemiological evidence suggests that populations who consume high levels of n-3 PUFA have reduced levels of chronic inflammatory or autoimmune diseases (30). While

many potential mechanisms are described below to explain the role of n-3 PUFA in inflammation, clinical trials show mixed results. For example, some studies show clinical benefit (31,32,33), while others failed to improve symptoms (34,35,36). This could be due to differences in dose, varying ratios of ALA, EPA and DHA, length of study, gender or age of the subjects (37,38) or other variables such as n-6 PUFA consumption, type of placebo (39), and the target condition of interest. Indeed, even within irritable bowel disease (IBD), Crohn's disease and ulcerative colitis often respond differently to n-3 PUFA treatment (39).

In preclinical studies, n-3 PUFA suppress inflammation by several mechanisms such as reducing inflammatory eicosanoids, cytokines and reactive oxygen species as well as increasing anti-inflammatory resolvins (40). In addition, fish oil decreases obesity-related inflammation by decreasing inflammatory hormones such as leptin and resistin while increasing anti-inflammatory adiponectin (41,42). Fish oil also modulates the genetic profile of adipose tissue and decreases $CD4^+$ T cell proliferation (22,43,44,45).

Recent evidence suggests that the anti-inflammatory effects of n-3 PUFA are relevant in humans. Maximal levels of membrane incorporation of EPA and DHA can be achieved within a week by consuming 2.4 g/d EPA and 1.2 g/d DHA (46,47). Dietary n-3 PUFA reduce inflammatory eicosanoid production which is replaced by anti-inflammatory or less active (48) n-3 derived eicosanoids (24,49) as well as n-3 PUFA derived resolvins E1 and D1 (50) which are involved in the resolution of inflammation through inhibition of neutrophil chemotaxis and IL-1β release (47). n-3 PUFA also modulate inflammatory gene expression (24) and macrophage activation in human

subjects (25). Recently, n-3 PUFA have been shown to reduce NF-κB activation in humans (51) possibly through PPARγ activation or GPR120 activation leading to reduced production of inflammatory cytokines (47). Finally, leukocyte chemotaxis (52), IL-6 (24) and T cell proliferation are reduced in humans (53).

### *Effect of n-3 PUFA on $CD4^+$ T cells*

n-3 PUFA modulate the immune response through effects on immune cell activation and abundance (23,41,54). $CD4^+$ T cells play an important role in the immune system by coordinating different cell reactions through cytokine action. During the acute phase of inflammation, $CD4^+$ T cell activation is critical for eliciting a functional response; however, excessive activation can lead to tissue damage. Enrichment of n-3 PUFA in murine cell membranes regulates $CD4^+$ T cell differentiation (23,41,54,55). Although mechanistic insights into the effects of n-3 PUFA on human $CD4^+$ T cells are limited, it has been shown that n-3 PUFA reduce ex vivo proliferation of $CD4^+$ T cells in humans (53) and this has been further probed in cell culture and animal studies. Specifically, n-3 PUFA reduce production of IL-2, a major stimulator of $CD4^+$ T cell proliferation (56) and gene expression of IL-2Rα (57). Furthermore, pro-inflammatory Th1 and Th17 cell in vivo abundance and differentiation ex vivo are reduced (23,41,54,55). Finally, inflammatory cytokines such as IL-17 and transcription factors such as ROR-γt are reduced by n-3 PUFA (41). One immunosuppressive mechanism of n-3 PUFA contributing to this effect may be linked to the IL-6 signaling pathway.

***Role of IL-6R and gp130 in IL-6 signaling***

The IL-6 receptor (IL-6R) is an 80 kDa surface protein expressed in monocytes, activated B cells and neutrophils as well as $CD4^+$ T cells, especially in the naïve or memory phenotypes (58). Downstream signaling by IL-6 is mediated through several steps, including both classical signaling and *trans*-signaling. During classical signaling, two molecules of IL-6 bind to two membrane bound IL-6 receptors (mIL-6R) which form a complex with two molecules of gp130 resulting in a hexameric signaling complex (**Figure 1,** 20,59). Interestingly, many cells, such as smooth muscle and endothelial cells (18), do not express IL-6R, yet they still exhibit *trans*-signaling in which soluble IL-6R (sIL-6R) shed from contiguous cells binds to IL-6 and membrane bound gp130. Typically, sIL-6R is produced by alternative splicing or enzymatic cleavage of mIL-6R by ADAM17 (a disintigrin and metalloproteinase) and ADAM10 (59,60,61). Activation of T lymphocytes with anti-CD3 and anti-CD28 leads to down regulation of IL-6R on the cell surface and an increase in sIL-6R (20,59) through the action of ADAM17; other activators of IL-6R shedding include PMA, bacterial metalloproteinases, C-reactive protein and cholesterol depletion (61). Elevated levels of sIL-6R seen during periods of inflammation are involved in the pathogenesis of rheumatoid arthritis, Crohn's disease and colon cancer (17,19,59). Indeed, sIL-6R appears to be responsible for the pathophysiology of IL-6 while mIL-6R is associated with normal cellular functions such as acute phase protein response and B cell modulation (18). gp130 is ubiquitously expressed and mediates signal transduction for

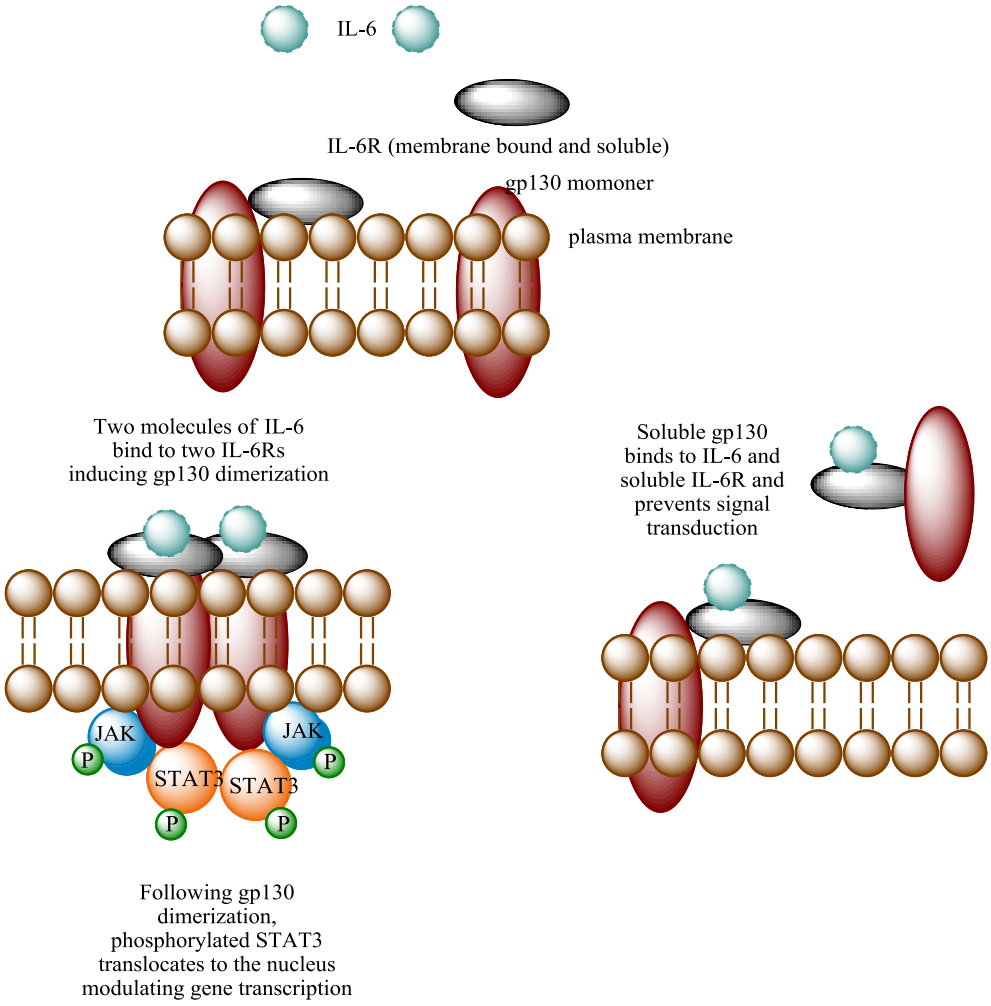


**Figure 1. IL-6 signaling through soluble and membrane bound receptors.** During classical signaling, two molecules of IL-6 bind to two membrane bound IL-6 receptors which induce gp130 homodimerization and downstream activation of the JAK-STAT pathway leading to translocation of ROR-γt to the nucleus to activate Th17 polarizing genes. During *trans*-signaling, soluble IL-6R binds to IL-6 and membrane bound gp130 to propagate signaling. Conversely, this pathway can be inhibited by soluble gp130 which prevents signal transduction.

IL-6 and many other cytokines including IL-11 and IL-27 (17). Similar to IL-6R, gp130 can be membrane bound (mgp130) or soluble (sgp130), where it activates JAK1, JAK2 and tyrosine kinase 2 (**Figure 1**). Soluble gp130 is produced by alternative splicing or proteolytic cleavage (62). Soluble gp130 acts as an inhibitor of IL-6 trans-signaling by binding to IL-6/sIL-6R without performing subsequent signal transduction (61). Mice engineered to be gp130 deficient die as embryos (17,58) suggesting that gp130 is essential for life. In $CD4^+$ T cells, a lack of gp130 leads to a reduced Th17 response and an increased Treg response, resulting in protection against experimental autoimmune encephalomyelitis (EAE) (17). The presence of soluble gp130 in the serum also inhibits Th17 development (20), suggesting that gp130 is an important mediator of Th17 differentiation.

***Effect of n-3 PUFA on the plasma membrane***

n-3 PUFA influence the structure of the plasma membrane (43,44), a highly heterogeneous lipid bilayer containing liquid ordered ($l_o$) and liquid disordered ($l_d$) regions (63,64,65). Liquid ordered regions, also known as lipid rafts, are enriched in cholesterol and sphingolipids and are insoluble in cold, nonionic detergents (65). These microdomains have been isolated and studied by detergent extraction and visualization by fluorescence microscopy. However, traditional fluorescence microscopy cannot visual individual rafts due to a diffraction limit of 200 nm. More recently, super-resolution microscopy techniques have been used to visualize individual raft domains that are sensitive to cholesterol depletion (64). These heterogeneous microdomains are

small (10-200 nm) and contain many signaling proteins. Raft domains, therefore, can function as a signaling platforms for many cell types (63,66). Indeed, previous research suggests that n-3 PUFA increase the condensation of lipid rafts around the immunological synapse. This effect is accompanied by a modification of the microenvironment or more specifically the proteins that are found within the raft and collectively these changes lead to reduced cellular activation (43). It has previously been shown that expression of membrane bound receptors including IL-6R is modulated by the cholesterol composition of the plasma membrane (67). This may be due to the fact that DHA is highly unsaturated and is therefore sterically incompatible with cholesterol, a major component of lipid rafts (68,69). This incompatibility affects the plasma membrane by altering membrane fluidity, phase behavior, permeability, fusion, flip-flop and protein function (69).

Previous research shows that reducing membrane glycosphingolipids blocks Th17 polarization without affecting other phenotypes (70) suggesting that Th17 polarization is modulated through a lipid raft related mechanism. These data suggest that by perturbing sites (domains) of high membrane dependent signaling, T cell activation is decreased. It has been shown that n-3 PUFA suppress the co-localization of T cell receptor signaling proteins into lipid rafts (43) which decreases the robustness of downstream signaling. With respect to IL-6 signaling, previous reports suggest that glycoprotein 130 is localized to lipid rafts in kidney (71) and neuroepithelial (72) cells, however, this has not been investigated in $CD4^+$ T cells. Since IL-6 is a critical initiator of Th17 differentiation, changes in the expression of members of the IL-6 signaling pathway can

drastically affect cell abundance. Indeed, a reduction in gp130 expression leads to significantly reduced Th17 abundance and a shift towards a Treg phenotype (17). Therefore, n-3 PUFA may decrease cellular responsiveness to IL-6 by altering the localization of gp130 in the plasma membrane.

***Significance***

It is currently unknown how n-3 PUFA modulate Th17 polarization. We have previously demonstrated that n-3 PUFA enhance lipid raft size in $CD4^+$ T cells leading to reduced cellular activation (69). Therefore, it is possible that lipid raft dependent IL-6R/gp130 Th17 polarization is disrupted by a similar mechanism. To determine the mechanism of n-3 PUFA action, *fat-1* transgenic mice were used as a genetic model of dietary n-3 PUFA.

The *fat-1* mouse contains the *fat-1* gene from *C. elegans* and is able to convert n-6 to n-3 PUFA in vivo and, therefore, can be used to study dietary n-3 PUFA without the need for a prolonged feeding period (21). *Fat-1* mice display a similar membrane enrichment of n-3 PUFA as a wild type mouse consuming a 4% fish oil diet (22). Furthermore, Th17 cell abundance is reduced in *fat-1* mice similar to dietary n-3 PUFA (23) suggesting that the genetic model is able to duplicate the phenotypic effect of a fish oil diet.

It is possible that EPA and DHA reduce responsiveness to IL-6 through a lipid raft related mechanism. This would result in the reduction of Th17 differentiation because n-3 PUFA modulate lipid raft mesodomains which contain components of the IL-6-gp130-

STAT3 axis. Therefore, our hypothesis was that n-3 PUFA reduce Th17 differentiation through disruption of gp130 localization in lipid rafts and further reduction in downstream signaling. In order to test this hypothesis, we examined the effects of n-3 PUFA on membrane localization of gp130, surface and gene expression of IL-6R and gp130, IL-6 induced gp130 dimerization and STAT3 phosphorylation in $CD4^+$ T cells from *fat-1* mice.

# METHODS

## *Experimental animals*

Male and female *fat-1* and wild type mice were obtained from Dr. Jing Kang, Harvard Medical School. Mice were bred at Texas A&M facilities, genotyped and phenotyped as described previously (73) and maintained on a modified AIN-76A diet containing 10% safflower oil (D03092902; Research Diets, New Brunswick, NJ) adequate in all required nutrients. Mice were maintained under barrier conditions with one to five mice per cage in a twelve hour light and dark cycle at 21°C. All procedures and protocols followed guidelines approved by the U.S. Public Health Service and the Institutional Animal Care and Use Committee at Texas A&M University.

## *$CD4^+$ T cell isolation & culture*

Wild type and *fat-1* mice were sacrificed by $CO_2$ asphyxiation and spleens were extracted aseptically and placed in sterile MACS buffer (Miltenyi Biotec, Auburn, CA). Spleens were crushed with a 10 mL syringe plunger through a 70 µm plastic mesh and washed with MACS buffer through a 40 µm filter (BD Falcon). The subsequent cellular suspension was applied to a Miltenyi positive selection column (See Appendix A for details). Viability was assessed by Trypan Blue exclusion and cell counts were determined by a Coulter counter before use in the following experiments. Cell stimulation was used for IL-6 induced dimerization or activation induced shedding of mIL-6R experiments (described below).

***Co-localization of gp130 in lipid rafts by immunofluorescence***

$CD4^+$ T cells were analyzed by immunofluorescence according to Kim et al (43) with some modifications. In order to determine activation-induced changes in gp130 and lipid rafts, $CD4^+$ T cells were activated with 0.17 µg/mL plate bound anti-CD3 and 1.67 µg/mL plate bound anti-CD28 (eBioscience) for 30 minutes at 37ºC and compared to an untreated control. For fluorescence experiments, comparison of fixation with paraformaldehyde (PFA) (Electron Microscopy Sciences) vs PFA plus glutaraldehyde (GA) (Sigma) was performed. Cells were fixed with 4% PFA alone or 4% PFA with 0.2% GA for 30 minutes at room temperature. For analysis of WT and *fat-1* cells, freshly isolated $CD4^+$ T cells were plated at 5 x $10^6$ per well for 30 minutes at 37ºC in poly-L-lysine coated chamber slides before fixation with 4% PFA for 30 minutes at room temperature. Quenching consisted of two consecutive 10 minute incubations with warm (37°C) 100 mM glycine followed by permeabilization with 0.2% Triton, blocking in 10% goat serum and overnight incubation in 10 µg/mL rat anti-mouse gp130 (R&D Systems, Minneapolis, MN). Following washing, cells were subsequently incubated with 10 µg/mL Alexa 555 conjugated donkey anti-rat IgG for two hours followed by incubation with 6 µg/mL Alexa 488 conjugated cholera toxin (Life Technologies, Carlsbad, CA) for one hour. Slides were dried in a series of ethanol and xylene washes before being coverslipped in ProLong antifade reagent (Molecular Probes) and subsequent visualization using a Zeiss 510 LSM in confocal mode. Co-localization appeared yellow due to red (Alexa 555) and green (Alexa 488) overlap which was quantitatively assessed by Pearson's correlation (43).

***Basal gp130 protein expression by western blot***

Basal levels of gp130 were assessed by western blot as described previously (69). To determine an optimal protein mass to load for the western blot, 1, 2, 4 and 8 µg of T cell lysate protein were applied to a 4-20% Tris-glycine gel (Expedeon) before being electrophoresed at 125 V for 2 hours followed by a 90 minute transfer onto a polyvinylidene difluoride membrane (Immobilon) at 400 mAmps. A quantity of 0.1 µg/mL rabbit anti-gp130 (Santa Cruz) was applied overnight followed by 0.1 µg/mL peroxidase labeled goat anti-rabbit IgG (KPL) for one hour to detect gp130. Chemiluminescence was quantified using Quantity One software (Bio-Rad) on a Fluor-S Max MultiImager (Bio-Rad, Hercules, CA) as described previously (69). For analysis of WT and *fat-1* protein expression, 4 µg of protein lysate was selected and processed.

***Quantification of gp130 and IL-6R mRNA by qPCR***

$CD4^+$ T cells were isolated for RNA extraction using an RNAqueous kit (Life Technologies, AM1914) according to the manufacturer's instructions followed by qPCR analysis as described previously (23). Briefly, freshly isolated splenic $CD4^+$ T cells were washed in PBS and suspended in Lysis/Binding buffer before addition of 64% ethanol. This suspension was applied to a spin filter and centrifuged at 13,000 rpm for 30 seconds before three washes with kit wash buffer 1 and wash buffer 2/3 twice followed by centrifugation at 13,000 rpm for 30 seconds after each wash. Pre-warmed elution buffer was used to recover the RNA by centrifugation at 15,000 rpm for 30 seconds. RNA quality was measured using a Bioanalyzer with an RIN cut-off of 8.0 or greater.

Quantification was assessed on a NanoDrop spectrophotometer (Waltham, MA) before reverse transcription was performed. For reverse transcription, a mixture of 90 ng of RNA, 0.25 µl hexamers, 1.25 µl oligo dT and RNase free water to a volume of 14.75 µl was heated to 65ºC for 5 minutes and cooled slowly to room temperature. The mixture was incubated at 37ºC for one hour with Superscript reverse transcriptase (Invitrogen), $1^{st}$ strand buffer, dithiothreitol, dNTPs and RNase inhibitor. After incubation, the mixture was frozen before further analysis by real-time PCR in which a TaqMan pre-developed assay from Life Technologies was utilized. In order to determine the optimal RNA mass for reverse transcription, 0.09, 0.9, 9, 90 and 900 µg of RNA were reverse transcribed and analyzed by qPCR as described in the Methods and the optimal concentration was determined by evaluation of the $C_T$ curves.

***gp130 and IL-6R surface expression by flow cytometry***

The antibody concentration was determined by selecting the optimal signal to noise ratio. Two hundred thousand freshly isolated splenic $CD4^+$ T cells were stained with either anti-gp130 or anti-IL-6R or the appropriate isotype control (BD Pharmingen) and the signal to noise ratio was determined by dividing the fluorescence intensity of the antibody stained cells by the fluorescence intensity of the isotype control stained cells and the highest ratio was selected for use. For analysis of WT and *fat-1* cells, $CD4^+$ T cells were stained with 1 µg CD 16/32 (Ebioscience) for 15 minutes at 4ºC and 0.5 µg anti-gp130 or anti-IL-6R (R&D and BD Bioscience, respectively) for 30 minutes on ice and analyzed on an Accuri flow cytometer. For activation induced shedding, cells were

stimulated in a 96 well plate with 5 µg/mL anti-CD3 and anti-CD28 (Ebioscience) for 48 hours at 37°C followed by analysis of surface expression by flow cytometry. Supernatants were stored at -80°C for analysis of soluble receptors by ELISA.

***Detection of sIL-6R by ELISA***

Soluble IL-6R was measured by ELISA (R&D Systems). In order to generate a threshold level of sIL-6R that could be read by the ELISA kit, $9x10^4$, $1.8x10^5$, $3.6x10^5$ and $7.2x10^5$ $CD4^+$ T cells were incubated for 48 hours in the presence or absence of stimuli before the supernatant was analyzed by ELISA. The incubation period was also optimized when $2x10^5$ cells were incubated with or without anti-CD3, anti-CD28 and TNF-α proteinase inhibitor (TAPI) for 24, 48 and 72 hours at 37ºC before analysis by ELISA. Supernatants were isolated and aliquoted after activation with anti-CD3 and anti-CD28 from above. In order to determine soluble receptor levels, supernatants were applied to a high binding 96 well plate (R&D Systems) previously coated overnight with 1.6 µg/mL IL-6R capture antibody and blocked with 1% BSA for one hour. Following a two-hour incubation with the supernatants, plates were washed and 200 ng/mL biotinylated goat anti-mouse IL-6R detection antibody was applied for 2 hours. Finally, the plate was incubated with horseradish peroxidase conjugated streptavidin followed by equal parts of 3,3',5,5'-Tetramethylbenzidine and hydrogen peroxide. The reaction was stopped with 2N sulfuric acid and the plate was read at 450 nm. Optical density at 540 nm was subtracted from the optical density at 450 nm before sIL-6R concentration was calculated to account for imperfections in the plate and give a more accurate reading.

***IL-6 induced gp130 dimerization by western blot***

Levels of gp130 dimer were also assessed as previously described (69). Briefly, $7x10^6$ $CD4^+$ T cells were stimulated with 100 ng/mL recombinant IL-6 (Biolegend 575704) for 15 minutes at 37°C followed by crosslinking in 3 mM bis(sulfosuccinimidyl)suberate (Thermo Scientific 21585) for 2 hours at 4°C. Samples were homogenized as described previously (69) and electrophoresed at 125 V for 3 hours followed by an overnight transfer onto a PVDF membrane at 400 mAmps. The gp130 monomer appeared at 130 kDa while the dimer appeared at 260 kDa. The protein levels were quantified by chemiluminesence as described above.

***IL-6 induced STAT3 phosphorylation by ELISA***

Freshly isolated $CD4^+$ T cells were stimulated with 50 ng/mL recombinant IL-6 for 15 minutes or 60 minutes. A cell population of $1x10^6$ cells per well were incubated in a 96-well plate (BD Falcon) at room temperature during stimulation followed by release of STAT3 in Cell Lysis Mix provided by the kit over shaking at 300 rpm for 10 minutes at room temp. Supernatants were used for STAT3 and phospho-STAT3 assessment using an ELISA kit from eBioscience (85-86103) according to the manufacturer's instructions. Briefly, 50 µl of sample was added to each well before addition of 50 µl total or phospho-STAT3 (Tyr705) antibody. After the mixture was incubated for 1 hour at room temperature with gentle shaking, each well was washed and 100 µl 3,3',5,5'-Tetramethylbenzidine plus hydrogen peroxide was added for 10-30 minutes. The

reaction was stopped with 100 µl 2N sulfuric acid before the plate was read on a spectrophotometer at 450 nm.

***Statistical analyses***

Graphpad Prism (La Jolla, CA, version 6) was used to analyze experimental data using the Student's t test for direct comparison of two populations or one-way ANOVA for multiple treatment groups with an upper limit of significance at $p<0.05$. Data not fitting a normal distribution (assessed using Graphpad Prism) was analyzed using the Mann-Whitney test.

# RESULTS

## *n-3 PUFA reduce co-localization of gp130 in lipid rafts*

Due to recent evidence demonstrating that lipid rafts are important for $CD4^+$ T cell activation (66,74), localization of gp130 in the plasma membrane was assessed by immunofluorescence. In order to determine the optimal method for fixation, freshly isolated, wild type $CD4^+$ splenic T cells were fixed with 4% PFA or 4% PFA plus 0.2% GA for 30 minutes before analysis by confocal microscopy (**Figure 2**). Cells were stained for gp130 (left column) and cholera toxin subunit B (CTxB), a lipid raft marker (middle column). The green signal from gp130 and the red lipid raft signal were overlaid (right column) to visualize co-localization as well as non-specific autofluorescence. While cells fixed with 4% PFA (top row) predominantly displayed membrane bound signal, cells fixed with PFA and GA (bottom row) displayed high levels of cytosolic fluorescence suggesting autofluorescence. For this reason, GA was not included in the fixation process. After fixation with 4% PFA, WT and *fat-1* splenic $CD4^+$ T cells were visualized using confocal microscopy (**Figure 3**). Lipid rafts were labeled with Alexa 488 conjugated CTxB (left column) while gp130 was labeled with Alexa 555 (middle column) and the two signals were overlaid (right column). The isotype control (top row) showed very little signal compared to WT cells (middle row) and *fat-1* cells (bottom row) labeled with anti-gp130 suggesting very low nonspecific binding in comparison with anti-gp130 stained cells. Pearson's correlation was used to quantitatively determine co-localization between gp130 and lipid rafts using a mathematical equation relating the

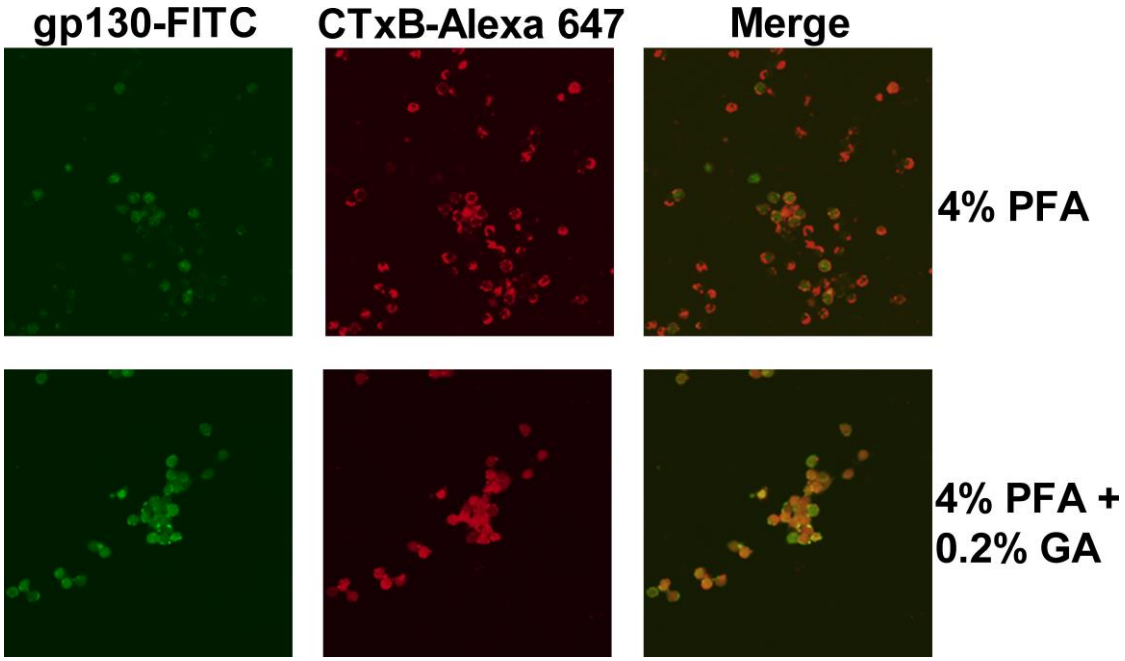


**Figure 2. Optimization of cell fixation for immunofluorescence.** Freshly isolated $CD4^+$ T cells were fixed with 4% PFA with or without 0.2% GA. The reaction was quenched with 100 mM glycine before cells were permeabilized with Triton and labeled with anti-gp130 and CTxB.

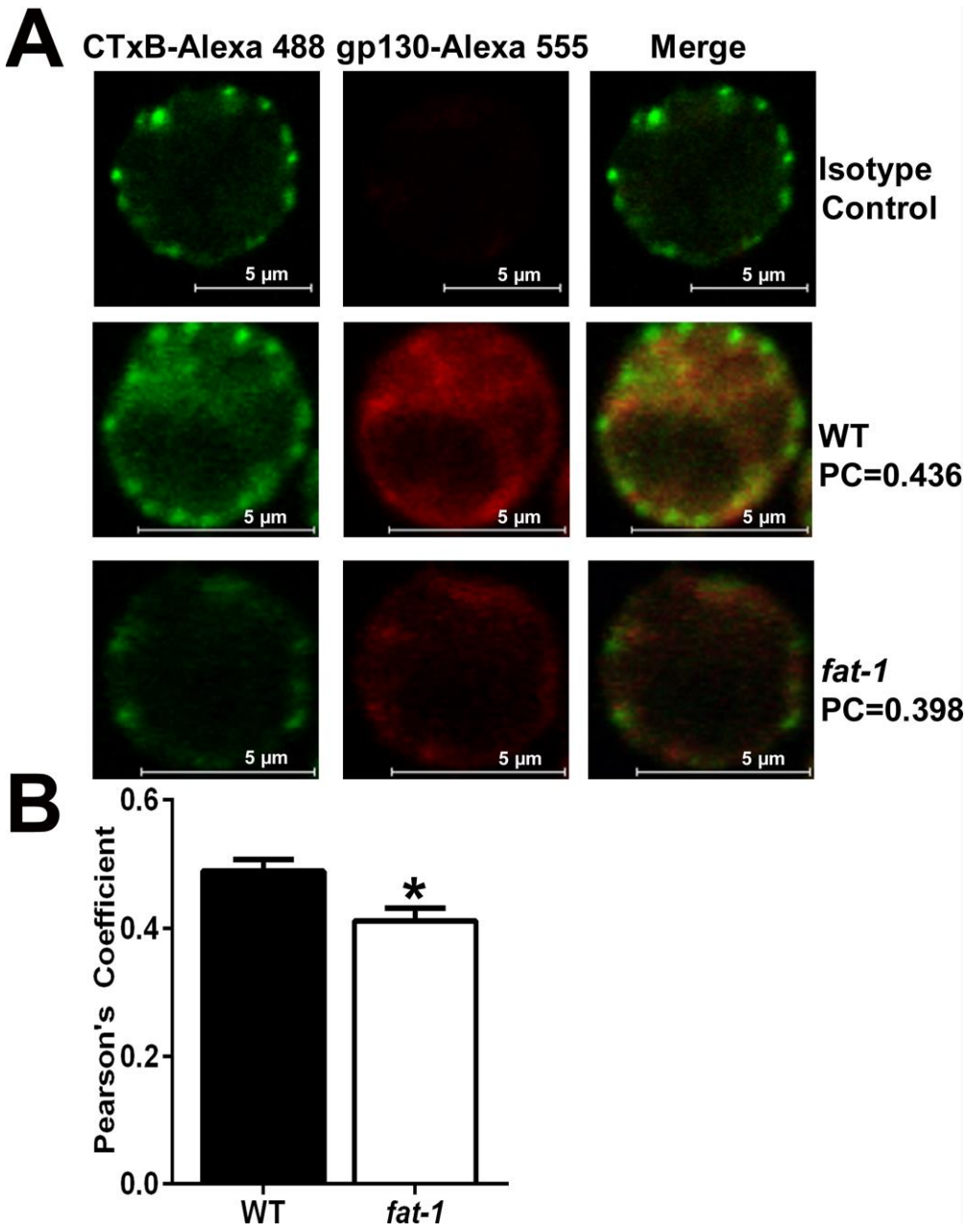


**Figure 3. n-3 PUFA displace gp130 from lipid rafts.** After fixation with 4% PFA, splenic $CD4^+$ T cells were quenched with 100 mM glycine followed by incubation with 2.7 µg/mL rat anti-gp130 or rat $IgG_{2A}$ overnight and 5 µg/mL Alexa 555 conjugated goat anti-rat IgG plus 3 µg/mL Alexa 488 conjugated CTxB for one hour before images were captured in confocal mode. A) Representative isotype control, WT and *fat-1* images B) Pearson's Correlation Coefficient (PCC) in WT vs *fat-1* derived cells. Data represent means ± SEM, n = 80 cells from 4 WT mice and 60 cells from 3 *fat-1* mice from three separate experiments.

intensity of each fluorophore in every pixel (75). *Fat-1* mice (bottom row) displayed reduced co-localization of gp130 and CTxB compared to WT mice (bottom row, p=0.004)

***n-3 PUFA do not affect surface or total cell expression of gp130***

Optimal antibody mass for measuring gp130 expression by flow cytometry was determined by signal to noise ratio. Representative histograms are shown for each antibody concentration compared to the isotype control (**Figure 4A**). A signal to noise ratio was determined for each concentration by dividing the fluorescence intensity of the antibody labeled cells by the fluorescence intensity of the isotype control (**Figure 4B**). An antibody concentration of 5 µg/mL was selected due to a high signal to noise ratio. Surface expression of membrane bound gp130 was assessed by flow cytometry in freshly isolated WT and *fat-1* splenic $CD4^+$ T cells. n-3 PUFA had no effect on the total number of cells expressing gp130 (**Figure 5A**). A representative histogram is also shown to compare gp130 fluorescence intensity between WT (black) and *fat-1* (red) $CD4^+$ T cells (**Figure 5B**). Quantibrite-PE beads (BD Scientific) were used to assess antibodies bound per cell (ABC) which was calculated by creating a standard curve of fluorescence intensity from the beads and converting the fluorescence intensity of each sample to the antibodies bound per cell. n-3 PUFA had no effect on the antibodies bound per cell or the average fluorescence intensity (**Figure 5E**). Subsequently, gene expression was assessed at both the mRNA and protein levels. Prior to analysis of WT and *fat-1* cells, differing levels of cell protein were analyzed in WT splenic $CD4^+$ T cells by western

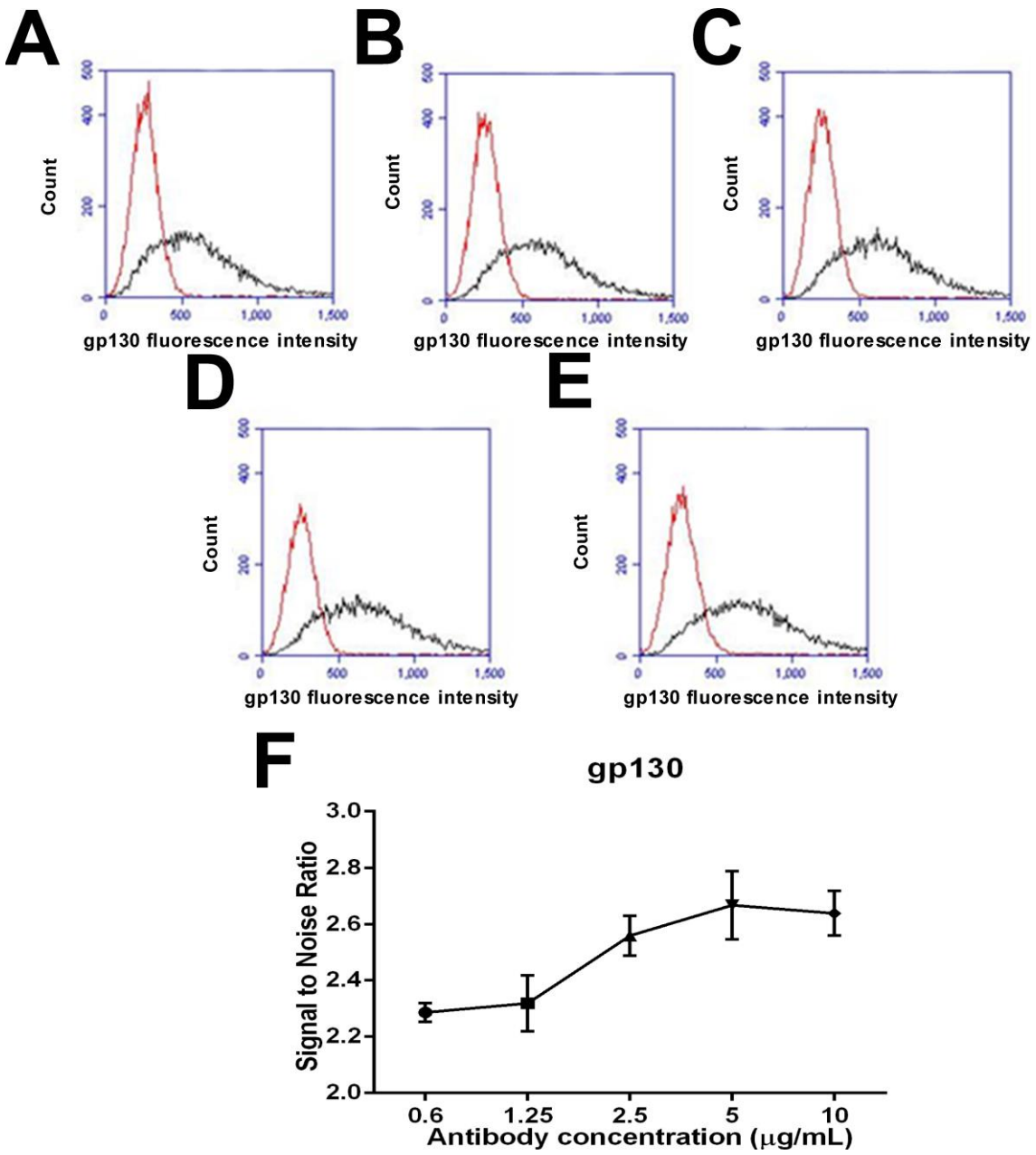


**Figure 4. Optimization of gp130 antibody level**. Splenic $CD4^+$ T cells were incubated with 0.6, 1.25, 2.5, 5 or 10 μg/mL anti-gp130 or anti-rat IgG (n=2-3 per treatment) for 30 minutes for analysis by flow cytometry. The signal to noise ratio was determined by dividing the fluorescence intensity in the anti-gp130 labeled cells by the fluorescence intensity in the isotype control with the same level of antibody. A) Representative dot plots at each antibody mass and histogram of cells labeled with anti-gp130 (red) or the isotype control (black). B) Signal to noise ratio at each antibody mass.

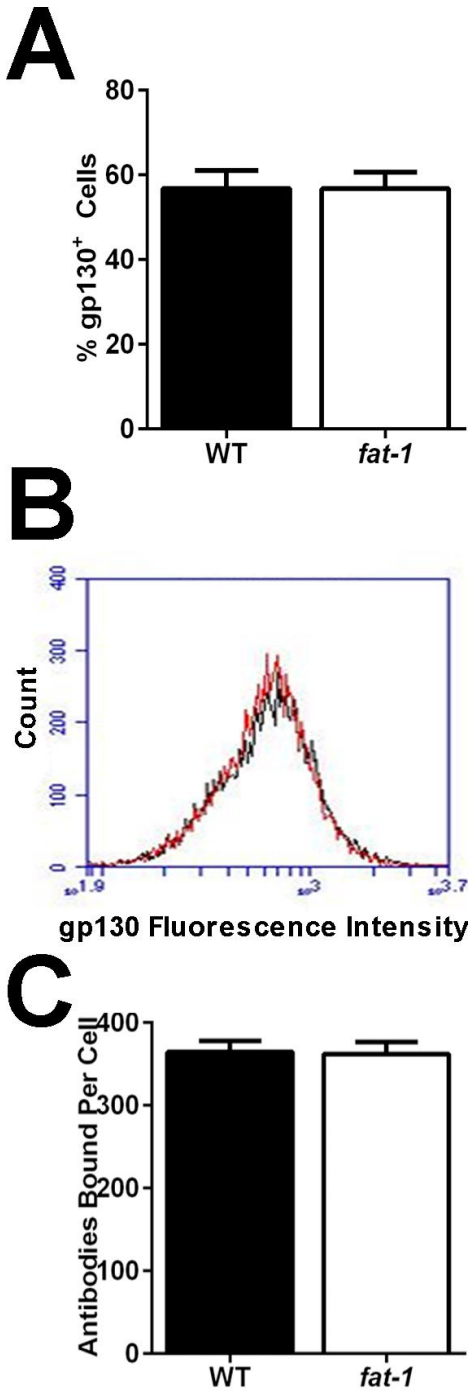


**Figure 5. Surface expression of gp130 is unaffected by n-3 PUFA.** Splenic $CD4^+$ T cells were isolated from WT and *fat-1* mouse spleens and stained with 2.5 µg/mL anti-gp130. A) and B) representative WT and *fat-1* images. C) Percentage $gp130^+$ cells, D) Overlay of WT (black) and *fat-1* (red). E) Antibodies bound per cell (ABC). Data represent mean ± SEM, n=4 mice.

blot to determine linearity in order to avoid over or under saturating the reaction between the anti-gp130 antibody and the gp130 protein (**Figure 6**). Protein levels of 1, 2, 4 and 8 µg were electrophoresed in duplicate (**Figure 6A**) and quantified by chemiluminescence (**Figure 6B**) and 4 µg of protein lysate was selected for analysis (**Figure 7A**) because this level was in the linear range of the reaction suggesting it was functioning most efficiently. Before WT and *fat-1* $CD4^+$ T cells were used for gene expression analysis, differing levels of RNA (0.09, 0.9, 9, 90 and 900 ng) were processed by reverse transcription to determine the linear region of the amplification reaction. An RNA mass of 90 ng was considered optimal (**Figure 8**). No change in gp130 total protein (**Figure 7B**) or mRNA (**Figure 7C**) was detected upon comparison of splenic $CD4^+$ T cells from WT and *fat-1* mice.

***n-3 PUFA reduce IL-6 induced gp130 dimerization and STAT3 phosphorylation***

In order to determine whether n-3 PUFA affect gp130 function, gp130 dimerization was induced in freshly isolated splenic $CD4^+$ T cells by incubation with 100 µg/ml recombinant mouse IL-6. After cross-linking with $BS^3$, the reaction was quenched with glycine and the cells were processed by western blot in the same manner as basal gp130 with the following modification. Seventeen micrograms of protein were electrophoresed for two hours with an overnight transfer to a PVDF membrane. During an optimization step, cells were either stimulated with IL-6 or left in resting conditions and duplicated with or without $BS^3$ for cross-linking (**Figure 9A**). For analysis of WT and *fat-1* cells, stimulated cells were compared to unstimulated cells from the same animal (**Figure 9B**)

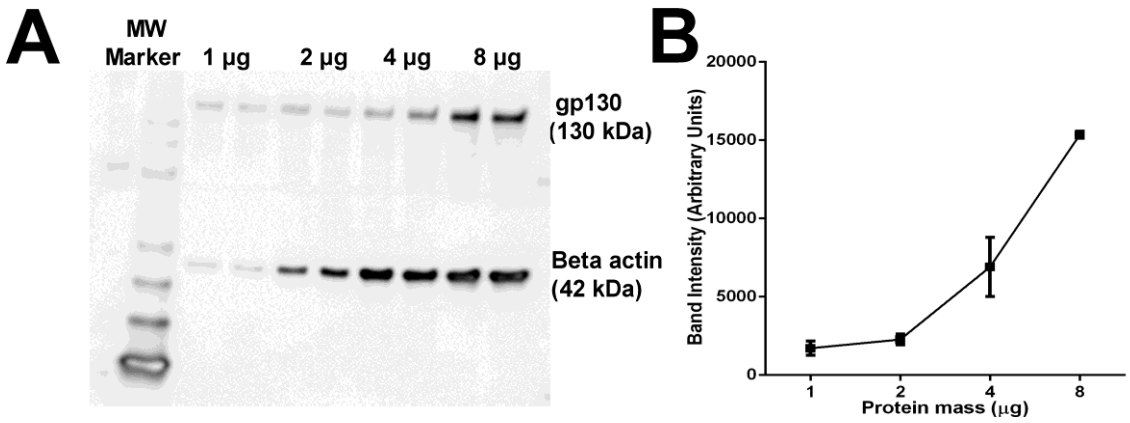


**Figure 6. Optimization of protein loading for western blot.** $CD4^+$ T cells were homogenized and protein was quantified using the Coomassie Plus Protein Assay. Varying amounts of protein (1, 2, 4 and 8 µg) were loaded into a 12% polyacrylamide gel and electrophoresed for 2 hours before transfer to a PVDF membrane for 1.5 hours. gp130 and beta actin were detected using antibodies from Santa Cruz and Abcam and detected by chemiluminescence. A) Representative image of a gel B) Fluorescence intensity by protein mass. Each data point represent mean ± SEM, n=2.

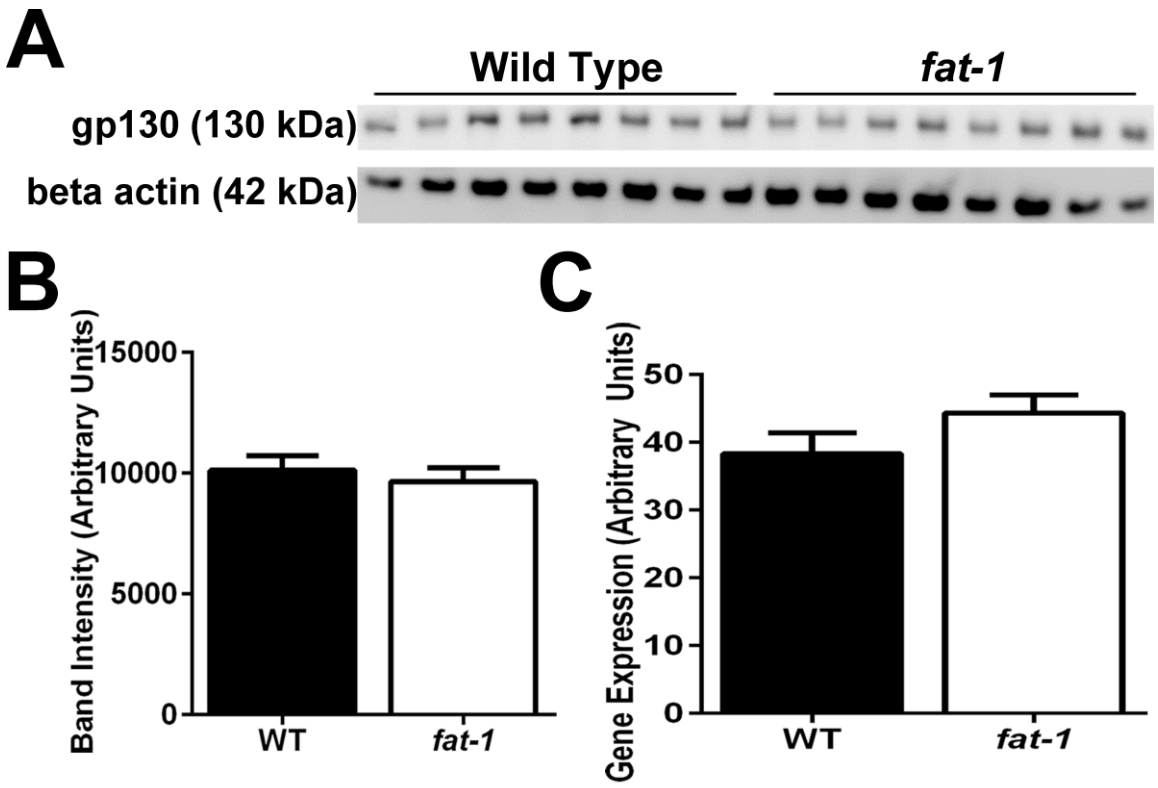


**Figure 7. Basal expression of gp130 and gene expression are not affected by n-3 PUFA.** A) $CD4^+$ T cells were isolated from wild type and *fat-1* mouse spleens and homogenized before lysates were assessed by western blot, n=8. B) gp130 levels in WT and *fat-1* mice. Data represent means ± SEM. C) gp130 gene expression was measured by qPCR, data represent means ± SEM, n=5-9.

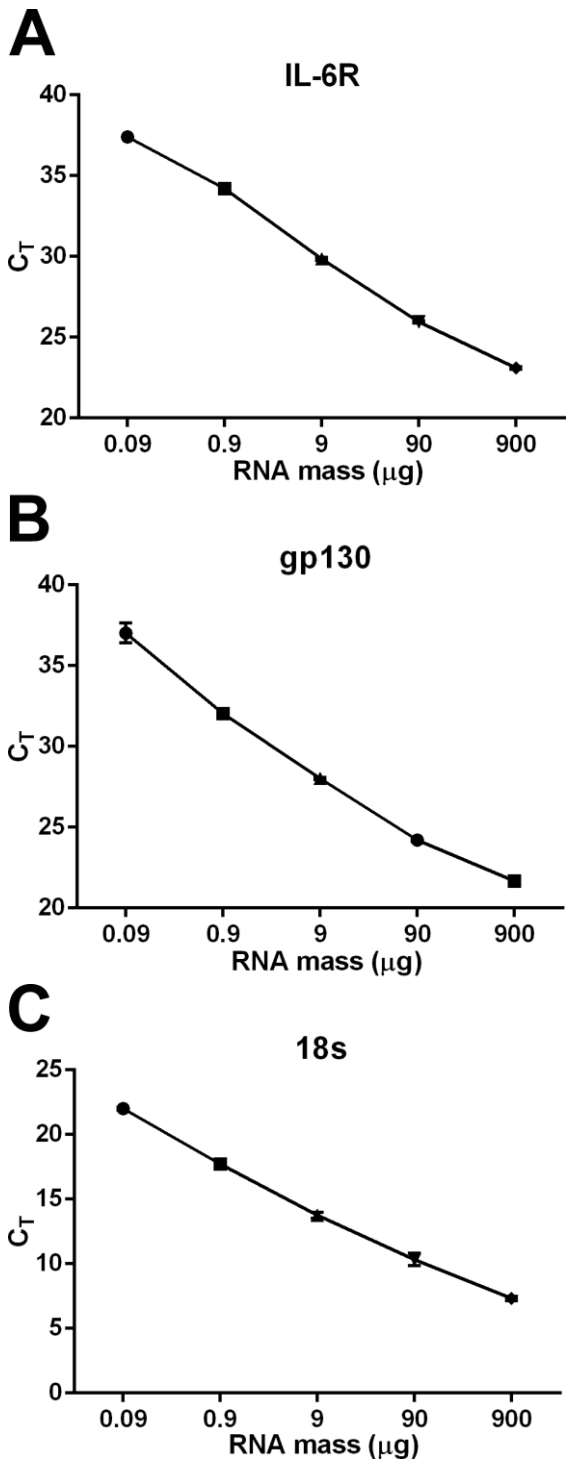


**Figure 8. Threshold cycle by RNA mass.** Differing levels of RNA were reverse transcribed and gene expression of A) IL-6 B) IL-6R C) gp130 and D) ribosomal 18s were analyzed by qPCR. Data represent mean ± SEM, n=4.

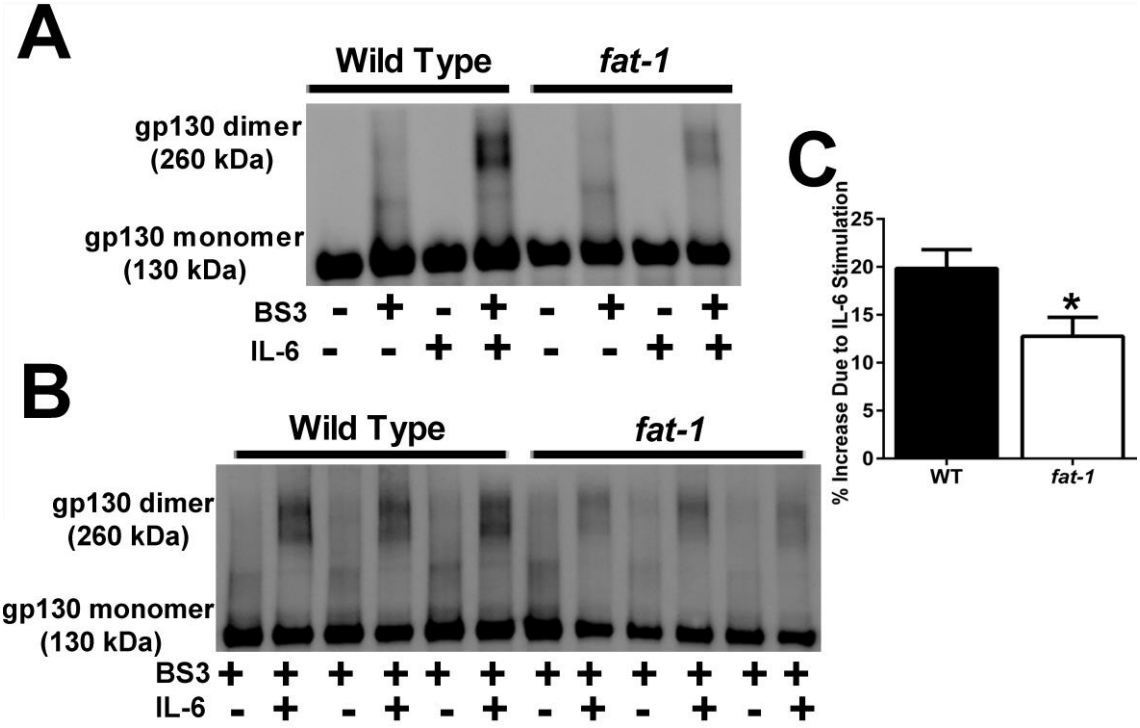


**Figure 9. n-3 PUFA reduce IL-6 induced gp130 dimerization**. $CD4^+$ T cells were stimulated with 100 ng/mL IL-6 to induce homodimerization of gp130 and subsequently cross-linked with $BS^3$. Negative controls for IL-6 and $BS^3$ are shown. A) Positive (+$BS^3$, +IL-6) and negative (-$BS^3$, – IL-6) controls. B) Representative image of WT and *fat-1* immunoblot ± IL-6. C) IL-6 induced dimerization was decreased in *fat-1* mice. Data represent means ± SEM of three separate experiments, and were normalized to individual unstimulated values, n=5.

to determine a percent increase due to stimulation. $CD4^+$ T cells from *fat-1* mice exhibited 35% reduced dimer formation (p=0.032) (**Figure 9C**). To further ascertain the functional status of the IL-6/gp130/STAT3 axis in the $CD4^+$ T cells from *fat-1* mice, STAT3 phosphorylation was assessed following stimulation by 50 μg/ml of IL-6. $CD4^+$ T cells from *fat-1* mice exhibited a 30% reduction in STAT3 phosphorylation in response to IL-6 (**Figure 10**) after 15 minutes (p=0.0014) and 60 minutes (p=0.0162) of stimulation.

***n-3 PUFA reduce surface IL-6R expression***

An optimal antibody concentration for IL-6R was determined as above and 5 μg/mL was selected for analysis. **Figure 11A-E** show histograms of fluorescence intensity for each antibody concentration compared to the isotype control. Each condition was conducted in triplicate and signal to noise ratios for each concentration were determined (**Figure 11F)**. Surface expression of membrane bound IL-6R was assessed by flow cytometry in freshly isolated WT and *fat-1* splenic $CD4^+$ T cells. Representative scatterplots of flow cytometric analysis are shown (**Figure 12A and B**) based on side scatter (y-axis) and IL-6R fluorescence intensity (x-axis). Splenic $CD4^+$ T cells from *fat-1* mice displayed a 30% reduction in the percentage (p=0.023) of IL-6R expressing cells (**Figure 12C**). In order to determine the cause of this decrease, shedding of IL-6R into $9x10^4$, $1.8x10^5$, $3.6 \times 10^5$ and $7.2 \times 10^5$ WT $CD4^+$ T cells were incubated with anti-CD3 and anti-CD28 for 48 hours and the supernatants were collected for analysis of sIL-6R the media under activating conditions was measured by ELISA. Initially, a range of by

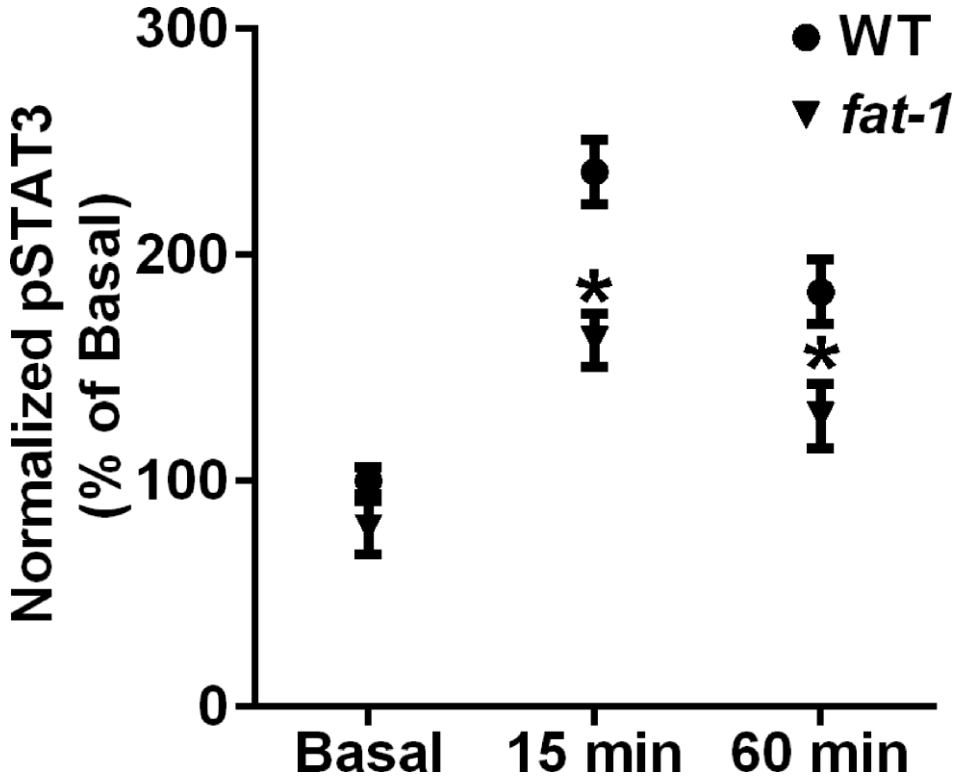


**Figure 10. n-3 PUFA reduce STAT3 phosphorylation**. $CD4^+$ T cells were incubated with 50 ng/mL IL-6 for 0, 15 and 60 minutes prior to homogenization. Cell lysates were analyzed by western blot for phospho-STAT3 and total STAT3, n=4. Data represent mean ± SEM. *Statistically different from WT ($p<0.05$).

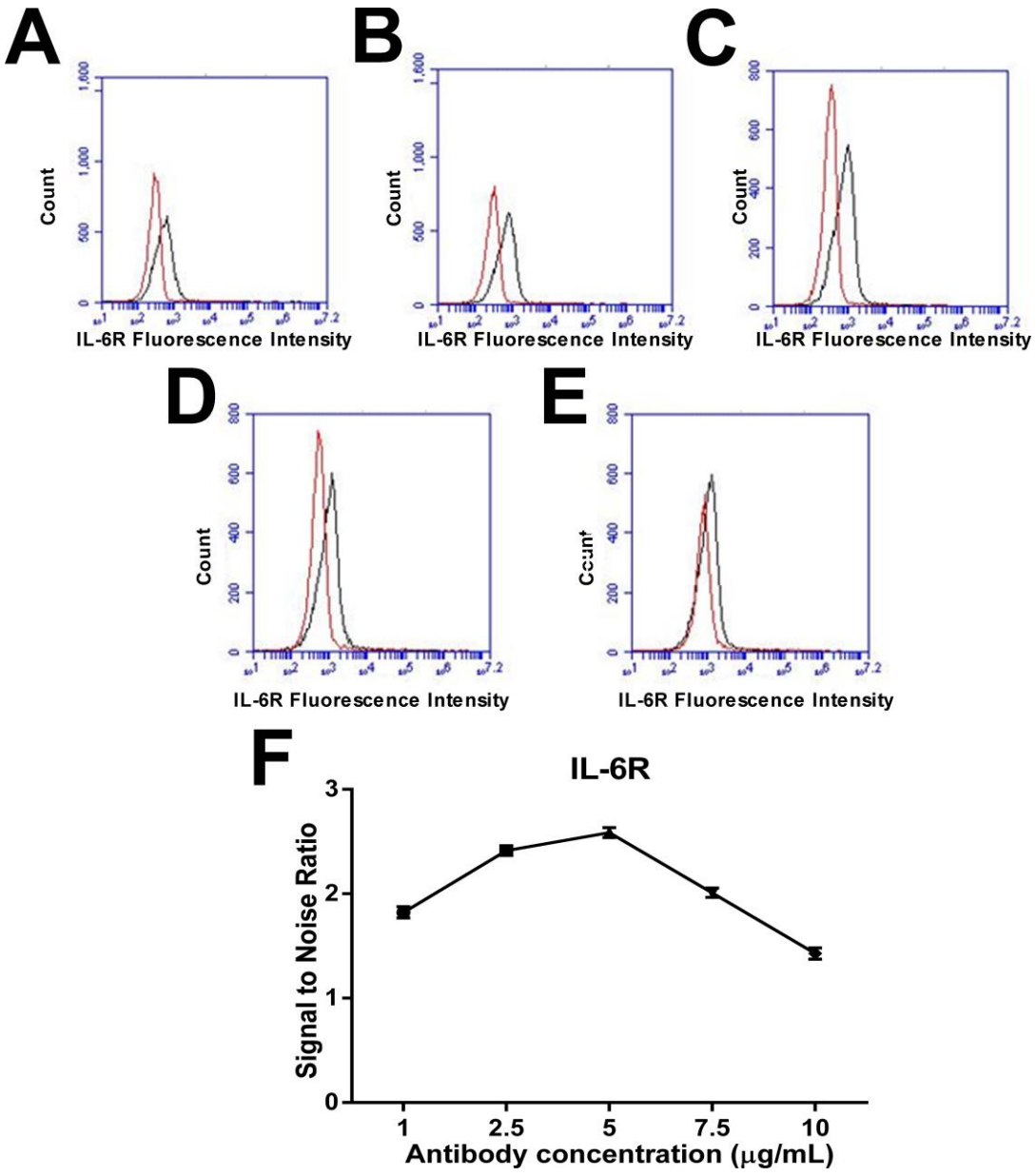


**Figure 11. Optimization of anti-IL-6R level.** Splenic WT $CD4^+$ T cells were incubated with A) 1 μg/mL B) 2.5 μg/mL C) 5 μg/mL D) 7.5 μg/mL or E) 10 μg/mL anti-IL-6R-PE for 30 minutes before analysis by flow cytometry. F) Signal to noise ratio by antibody concentration from one experiment, n=3 per treatment. Data represent mean ± SEM.

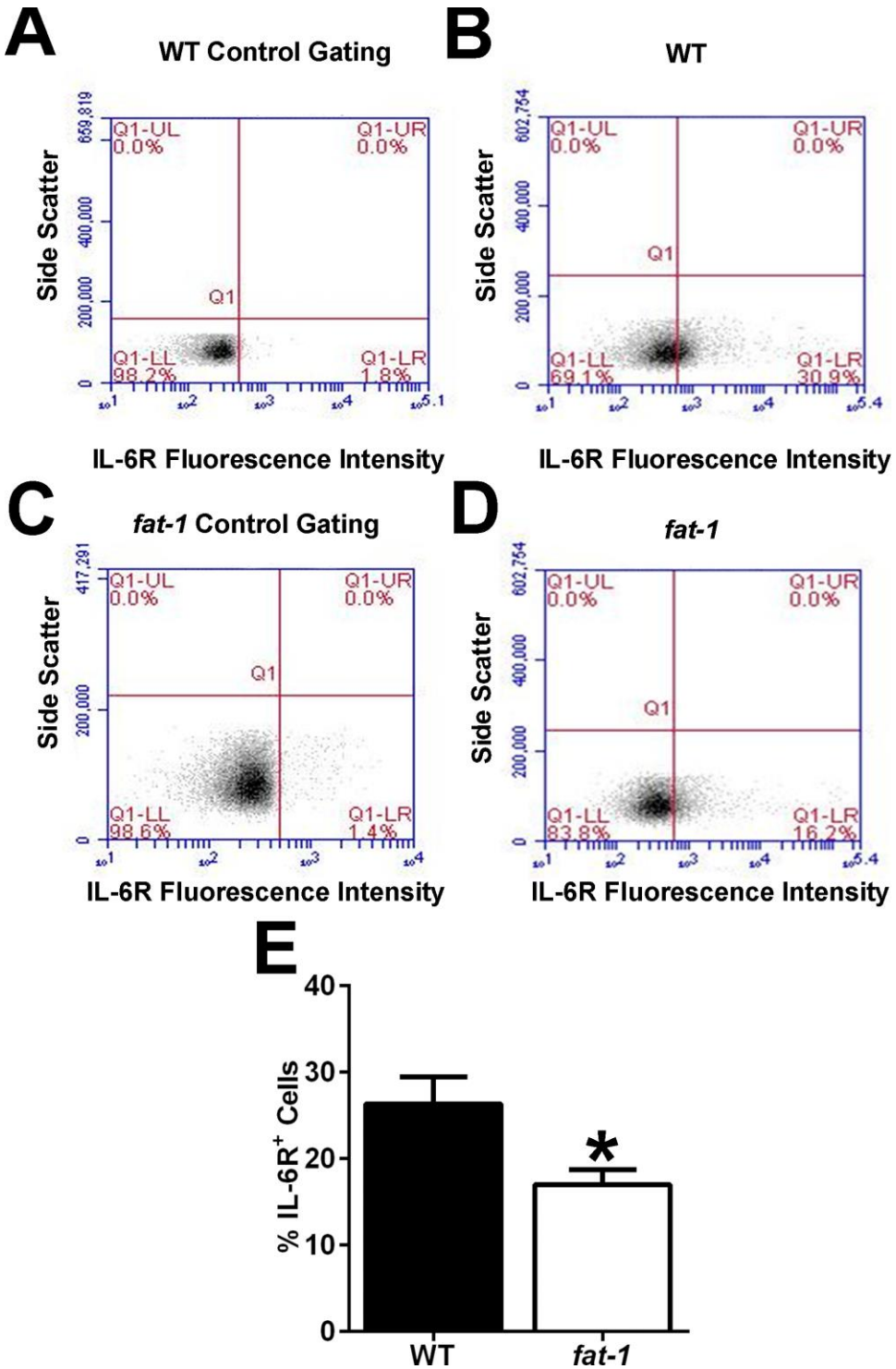


**Figure 12. Surface expression of IL-6R is decreased by n-3 PUFA.** Splenic $CD4^+$ T cells were isolated from WT and *fat-1* mice and stained with 5 µg/mL anti-IL-6R. A) and B) representative WT and *fat-1* images, respectively C) Overlay of WT (black) and *fat-1* (red). D) Percentage $IL\text{-}6R^+$ cells. Data represent mean + SEM, n=11.

ELISA. **Figures 13A** shows the concentration of sIL-6R (pg/mL) from each number of incubated $CD4^+$ T cells unstimulated, stimulated or stimulated with TNF-α protease inhibitor (TAPI) which inhibits α disintigren and metalloproteinase (ADAM) and therefore greatly reduces the shedding of IL-6R. As expected, stimulation of $CD4^+$ T cells led to an increase in soluble IL-6R detected in the culture media (**Figure 13A**) and TAPI decreased detectable sIL-6R in a cell population of $4 \times 10^6$ cells. This cell number was chosen because fewer cells yielded undetectable sIL-6R after treatment with TAPI and a higher level of cells increased apoptosis which is known to cause IL-6R shedding suggesting a non-specific result. Furthermore, an incubation time of 48 hours was selected as 24 hours did not yield an increase in sIL-6R upon cellular activation and 72 hours led to excessive apoptosis (**Figure 13B**). After analysis of WT vs *fat-1* cells, n-3 PUFA had no effect on basal, activated or TAPI treated sIL-6R levels (**Figure 14A**). To further probe the effect of n-3 PUFA on IL-6R expression, mRNA was isolated from naïve $CD4^+$ T cells and assessed by qPCR. Optimization was carried out as above. Gene expression did not differ ($p>0.05$) between WT and *fat-1* T cells (**Figure 14B**).

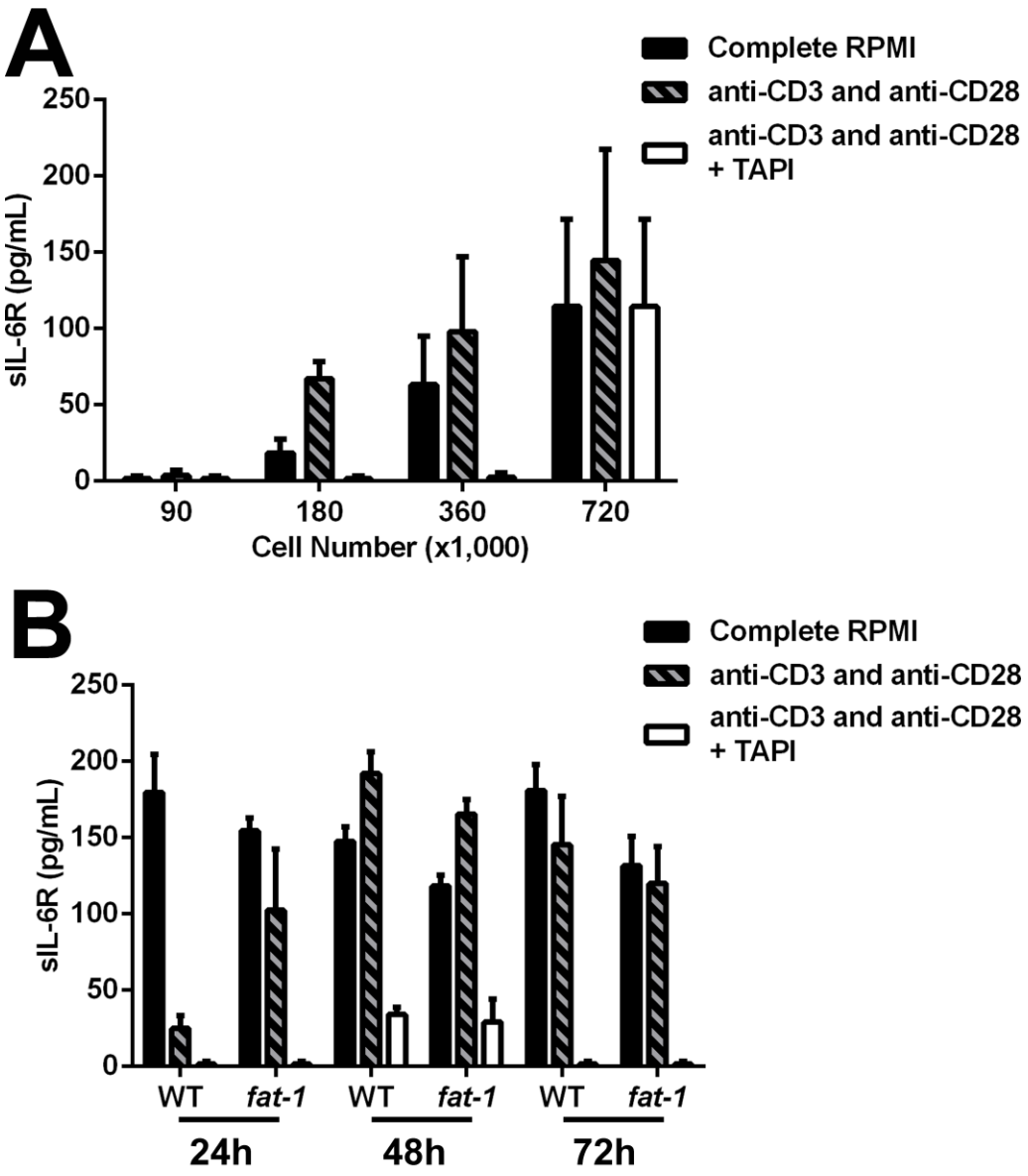


**Figure 13. Optimization of CD4$^+$ T cell activation and measurement of sIL-6R.** CD4$^+$ T cells were stimulated with anti-CD3 and anti-CD28 for 24, 48 and 72 hours before supernatants were collected and analyzed by ELISA. A) Comparison of varying amounts of WT CD4$^+$ T cells were incubated for 48 hours, data represent mean ± SEM, n=3 per condition.. B) A cell population of 4 x $10^6$ CD4$^+$ T cells from WT and *fat-1* mice were stimulated over 24, 48 and 72 hours. Data represent mean ± SEM, n=4 per condition.

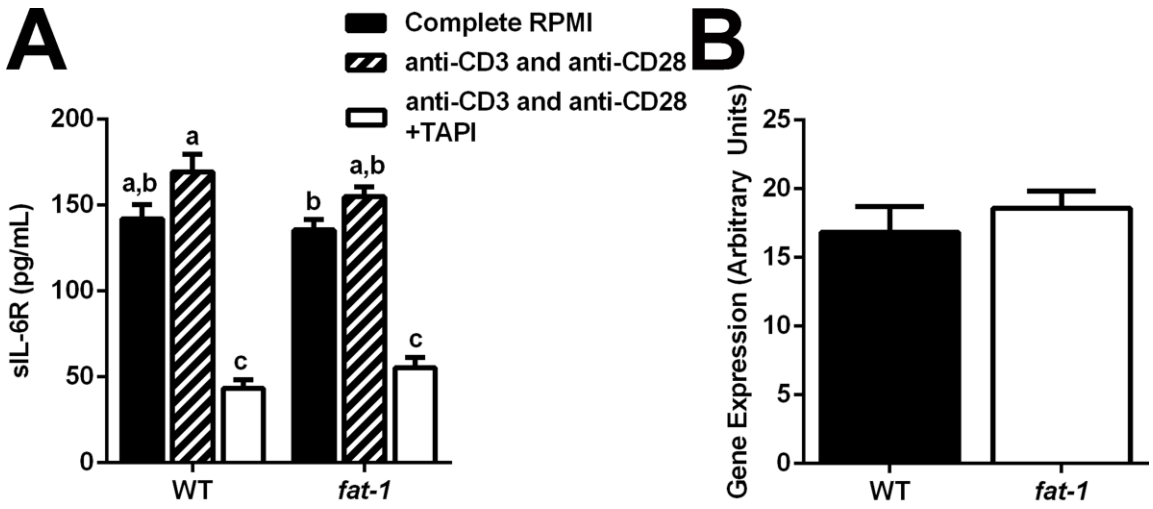


**Figure 14. Decreased surface IL-6R is not due to increased shedding or decreased transcription.** A) Soluble IL-6R was measured in the supernatant fluids from splenic CD4+ T cells activated with anti-CD3 and anti-CD28 for 48 hours. TAPI was used to inhibit shedding of IL-6R. Data are combined from two separate 48 hour incubations, n=8. B) IL-6R mRNA levels were measured by qPCR. Data represent means ± SEM, n=5-9.

# DISCUSSION

Uncontrolled inflammation is implicated in many of the current leading causes of death in the United States (2,3). Acute inflammation is a normal and healthy process involved in tissue repair and clearance of pathogens; however, if unresolved, chronic inflammation can lead to tissue damage, insulin resistance and disease such as arthritis, diabetes and inflammatory bowel diseases (1,2,3,15). Many dietary bioactive compounds appear to play a role in increasing or decreasing inflammation (76,77). One such anti-inflammatory dietary component is n-3 PUFA which reduce inflammation, in part, through altered eicosanoid metabolism (24,49). n-3 PUFA are incorporated into the plasma membrane at the expense of arachidonic acid and therefore are substituted as substrates for eicosanoid synthesis leading to anti-inflammatory products (24,78). Other mechanisms include modulation of inflammatory genes and production of anti-inflammatory lipid modulators such as resolvins and protectins (50,78). Most of these mechanisms have been assessed in a murine model; however, dietary interventions in humans indicate an increased production of anti-inflammatory resolvins (50) including resolvins E1 and D1 (50) and protectins (79). Resolvins and protectins are involved in resolution of inflammation through inhibition of neutrophil infiltration and production of IL-1β and TNF and are beneficial in inflammatory models such as colitis (47). Furthermore, eicosanoid metabolism is shifted from a reduction in proinflammatory eicosanoids (24,80) such as 2-series prostaglandins and 4-series leukotrienes (81), to an increase in less biologically active n-3 PUFA derived 3-series prostaglandins (82) and 5-

series leukotrienes (83) Additionally, dietary n-3 PUFA reduces inflammatory gene expression, e.g., IL-6, HIF1α and TGFβ1, and increases in anti-inflammatory adiponectin mRNA (24). TNF-α, IL-1β and IL-2 appear to be reduced while the anti-inflammatory cytokine IL-10 is increased by fish oil supplementation (84,85,86,87). In human neutrophils, n-3 PUFA reduce respiratory burst in older individuals (38) and superoxide generation in healthy volunteers (88). Furthermore, antigen presentation capability is reduced in human monocytes after fish oil supplementation (89). Finally, diets enriched in n-3 PUFA reduce T lymphocyte proliferation in response to the polyclonal mitogen Con A (53). These results suggest that n-3 PUFA are capable of acting upon the human immune system to favorably modulate immune activation and inflammation.

$CD4^+$ T effector cells e.g. Th1, Th2 and Th17 cells, are involved in stimulating the immune response for pathogen clearance, while $CD4^+$ regulatory T cells (Tregs) are involved in immune suppression after a threat is resolved or during an attack on host cells (90,91,92). Recent preclinical work has focused on Th1 and Th17 cells which mediate autoimmune and inflammatory conditions (9,90). For example, Th17 cells are associated with diseases such as arthritis, irritable bowel disease and multiple sclerosis (93) evidenced by elevated levels in the blood of IBD patients (94,95), as well as the blood and synovial fluid of patients with rheumatoid arthritis (96). Protection from experimental autoimmune encephalitis (EAE) (97), an animal model of multiple sclerosis is conferred in IL-6 deficient mice. This is significant because IL-6 is critical for Th17 development suggesting that EAE is dependent, in part, by a Th17 response.

Finally, IL-17 deficient mice are resistant to collagen-induced arthritis (92). With respect to diet, n-3 PUFA reduce systemic and local Th1 (54,98) and Th17 abundance as well as ex vivo differentiation of naïve $CD4^+$ T cells into a Th17 phenotype (23,41,55). While a reduction in Th17 differentiation by n-3 PUFA has not been confirmed in humans, clinical trials show a reduction in inflammatory cytokines including TNF-α (84), IL-1β (49), IL-2 (85) and IL-6 (24,86). Common anti-inflammatory treatments include non-steroidal anti-inflammatory drugs (NSAIDs) such as aspirin. These drugs are very effective in reducing pain by decreasing pro-inflammatory prostaglandin synthesis; however, negative side effects can also be present with the most common being gastrointestinal disturbances. For example, up to 40% of regular NSAID users may experience dyspepsia, nausea, vomiting, abdominal pain and heartburn and about 10% of long term users will have to stop treatment due to these effects (99). It is therefore necessary to determine innocuous dietary compounds that can reduce inflammation without causing negative side effects.

This study used transgenic *fat-1* mice which generate n-3 PUFA from n-6 PUFA *de novo* due to an n-3 fatty acid desaturase from *C. elegans* (21). These mice have been shown to incorporate n-3 PUFA into the plasma membranes of $CD4^+$ T cells to the same extent as mice on a 4% fish oil diet (100). These data suggest that the *fat-1* mouse faithfully recapitulates the phenotype seen in conventional mice fed an n-3 PUFA enriched diet and is therefore a valid model for the study of the effect of n-3 PUFA on T cell biology. A human equivalent dose for a mouse on a 4% FO diet was calculated as described previously (101). A 30 g mouse typically consumes 45 mg/d EPA + DHA

which is converted to 1500 mg/kg/d. This can be converted to a human dose using a $K_m$ factor determined by dividing weight by body surface area. The mouse $K_m$ factor, 3, was divided by the human $K_m$ factor, 37, and the subsequent number was multiplied by the 1500 mg/kg/d consumed by a mouse to get an average consumption by a human. This was multiplied by the average 70 kg human weight to achieve a human equivalent dose of 8.5 mg/d. This is much higher than the current 0.13-0.17 g/d EPA + DHA (28) consumed by Americans although it is lower than what is consumed by the Greenland Inuit, whose diet contains approximately 6 to 14 g/d n-3 PUFA including ALA, EPA and DHA (102,103).

Th17 effector cells require IL-6 and TGF-β for differentiation (5,104). IL-6 binds to membrane bound or soluble (IL-6R) which in turn binds to membrane bound gp130. Together with another IL-6/IL-6R/gp130, a hexameric signaling structure is formed and downstream signaling is accomplished through phosphorylation of JAK and STAT3 and subsequent dimerization of STAT3 before translocation to the cell nucleus and activation of ROR-γt, the master regulator of Th17 differentiation (60,105). Blockade of the IL-6R in vivo inhibits the development of a Th17 phenotype resulting in a protective effect in experimental autoimmune encephalitis (EAE) (106); this disease is also blocked by deletion of STAT3 (107) further suggesting that modulation of the IL-6-gp130-STAT3 signaling axis can affect inflammatory diseases by altering Th17 action.

Although it has been shown that n-3 PUFA reduce in vivo Th17 cell abundance and ex vivo differentiation, the mechanism is currently unknown. Based upon the evidence that membrane lipid raft modulation disrupts Th17 development (70), and that gp130, an

essential mediator of IL-6 signaling, localizes to lipid rafts (71,72), we hypothesized that n-3 PUFA reduce Th17 differentiation by interfering with IL-6 signaling in a lipid raft-dependent fashion. We therefore assessed gp130 expression at the cell surface, total protein and mRNA levels as well as the functional capacity of the signaling axis through gp130 dimerization and STAT3 phosphorylation. Measurement of surface IL-6R expression under basal conditions and following T cell activation were evaluated following incorporation of n-3 PUFA.

Currently there is disagreement regarding the exact mechanism by which n-3 PUFA acts on lipid rafts (108). DHA is sterically incompatible with cholesterol and would therefore be inserted into the bulk domain and enlarge lipid rafts by forcing cholesterol into raft domains. Differential scanning calorimetry and pressure-area isotherms experiments have supported this theory (109). However, this disagrees with evidence suggesting that DHA can be inserted directly into the lipid raft region based on quantitative microscopy techniques (110). It has been suggested that these opposing ideas can be combined wherein the addition of DHA to lipid rafts causes a structural segregation of DHA rich regions within the raft which are distinct from DHA poor regions. This segregation leads to rearrangement of proteins in or out of the raft region (108). By stabilizing lipid rafts at the immunological synapse, n-3 PUFA suppress the ability of signaling proteins to interact and effectively function as a signaling platform. Therefore, the first aim of this study was to measure the lipid raft localization of gp130, a critical co-receptor and signal transducer in the IL-6 signaling pathway. IL-6 and TGF-β are essential stimuli for Th17 differentiation (111) and previous studies

suggested that gp130 is localized in liquid ordered domains in kidney and neuroepithelial cells (71,72). We showed that n-3 PUFA did not affect mRNA, cellular (**Figure 7A, B, C**) or surface expression of gp130 (**Figure 5**). However, our results demonstrate that n-3 PUFA reduce localization of gp130 to lipid rafts (**Figure 3**). This is noteworthy, because lipid rafts act as signaling platforms for $CD4^+$ T cell activation and a decrease of gp130 localization in these mesodomains could lead to a reduction in signaling capacity.

gp130 homodimerization is a critical component of the IL-6-gp130-STAT3 axis and dimerization can be used as a functional measure of signaling capacity. For this reason, IL-6 induced gp130 dimerization was measured in the splenic $CD4^+$ T cells from WT and *fat-1* mice to determine if this critical step was disrupted by n-3 PUFA. *Fat-1* mice exhibited a highly significant ($p=0.032$) 35% reduction in gp130 dimerization (**Figure 9**), indicating that the functional ability of the protein is decreased. Furthermore, IL-6 induced STAT3 phosphorylation, a measure of signaling activity through the IL-6R/gp130 axis, was also significantly reduced ($p<0.05$) in $CD4^+$ T cells from *fat-1* mice (**Figure 10**).

This is the first report to document that the ability of n-3 PUFA to alter the membrane localization of gp130 in lipid rafts is associated with a reduction in IL-6 induced gp130 dimerization and STAT3 phosphorylation. We also observed a significant reduction ($p=0.023$) in the surface expression of IL-6R in the splenic $CD4^+$ T cells from *fat-1* mice which suggests a second, independent mechanism by which n-3 PUFA might interfere with differentiation of Th17 cells (**Figure 12**). There are a number of possible

mechanisms that might account for this reduction including increased receptor shedding upon cellular activation, reduced production of mRNA or total protein, receptor internalization or altered trafficking of the receptor to the cell surface. In this study, we determined that the reduction in in IL-6R surface expression was not due to increased shedding of IL-6R upon activation (**Figure 14A)** or a decrease in IL-6R mRNA production (**Figure 14B**). Future work will focus on elucidating the mechanism by which n-3 PUFA reduce IL-6R surface expression.

# CONCLUSIONS

**Figure 15** shows the mechanistic model for the suppression of Th17 differentiation by n-3 PUFA. A typical membrane contains liquid ordered (lipid rafts) and liquid disordered regions. gp130 is localized in both raft regions and non-raft regions. During basal conditions some IL-6 is present and IL-6R exists both in the membrane and in the plasma. With an n-3 PUFA diet, raft regions enlarge and become more stable. gp130 localization in lipid rafts is decreased leading to reduced dimerization and downstream activation of STAT3. Finally, membrane bound IL-6R is decreased without a subsequent increase in soluble IL-6R. These changes lead to reduced Th17 differentiation with n-3 enrichment. In summary, our results indicate two novel mechanisms by which n-3 PUFA interfere with Th17 differentiation in vivo and ex vivo. By reducing co-localization of gp130 in lipid rafts in the $CD4^+$ T cell membrane, n-3 PUFA attenuate the signaling capacity of the IL-6-gp130-STAT3 axis as evidenced by reduced gp130 dimerization and STAT3 phosphorylation (**Figure 15**). Furthermore, the ability of n-3 PUFA to reduce IL-6R surface expression is consistent with a decreased cellular responsiveness to this essential Th17-inducing cytokine. Our findings provide new insights into the mechanism by which n-3 PUFA suppress Th17 cell differentiation and add to the other mechanisms by which n-3 PUFA are known to suppress inflammation (78,112). Current anti-inflammatory treatments such as NSAIDS or glucocorticoids are expensive and often involve serious side effects (113,114). Given the high proportion of the population which is afflicted by inflammation; it is important to identify innocuous anti-

inflammatory dietary compounds that could ameliorate inflammatory conditions and improve the health of this population. n-3 PUFA reduce $CD4^+$ T cell activation and the pro-inflammatory differentiation and functions of effector Th1 and Th17 subsets (23,41,54,55). Understanding the precise mechanisms of these beneficial effects is critical to making informed decisions about recommendations for n-3 PUFA consumption in the diet or as supplements. This study has added new insights to that body of knowledge.

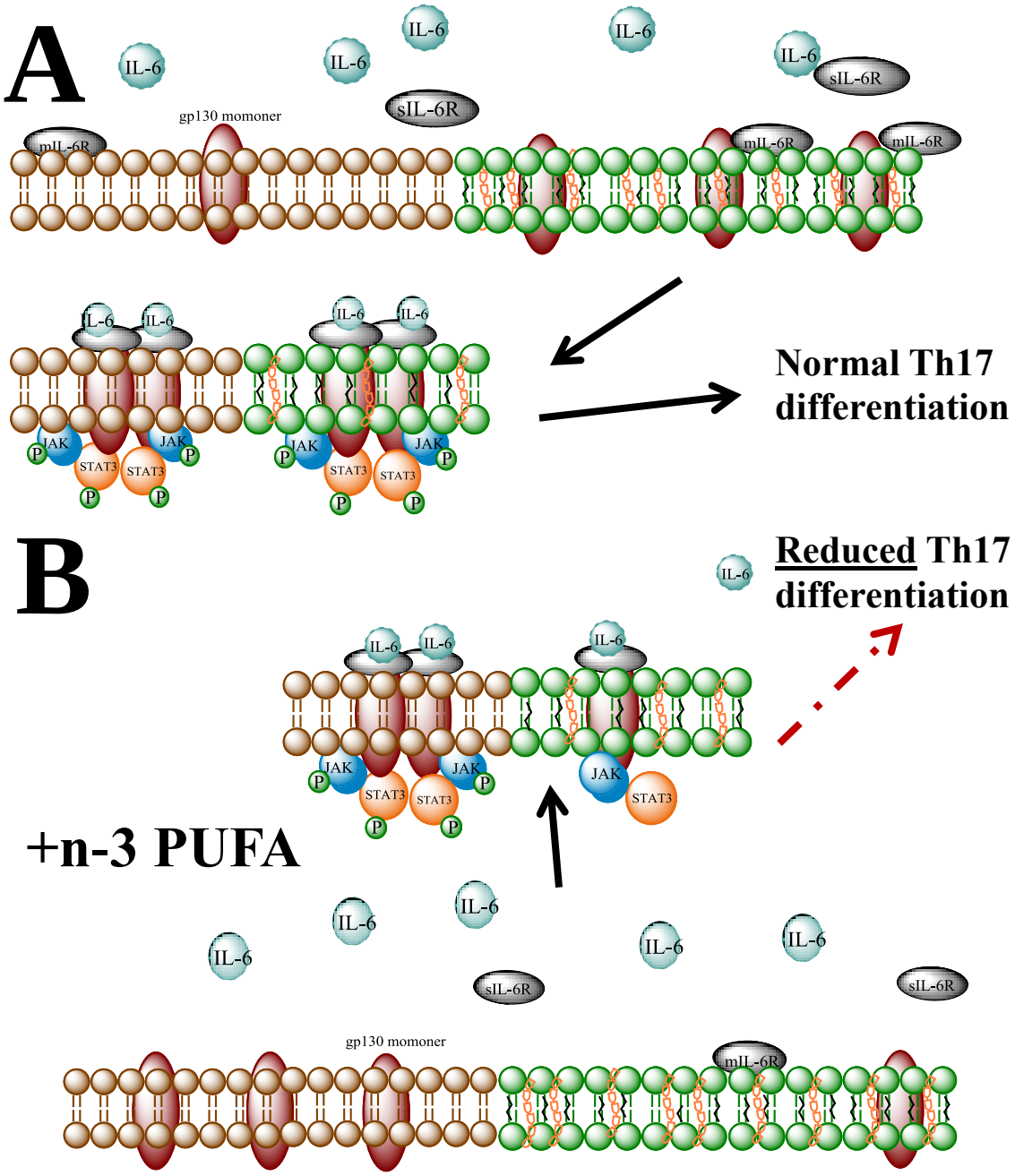


**Figure 15. Mechanistic model describing the effects of n-3 PUFA on Th17 differentiation.** The IL-6 signaling pathway is displayed in a cell membrane leading to Th17 differentiation. Different domains of the plasma membrane are denoted by color where brown is the bulk domain and green shows a lipid raft enriched in cholesterol (orange) and unsaturated fatty acids (black). A) In a WT mouse, IL-6 binds to IL-6R leading to gp130 dimerization and a hexameric signaling structure. Upon phosphorylation, STAT3 translocates to the nucleus to induce Th17 differentiation. B) In the *fat-1* mouse, n-3 PUFA reduce gp130 co-localization and surface IL-6R expression which lowers cellular responsiveness to IL-6, evidenced by reduced gp130 dimerization and STAT3 phosphorylation. This leads to reduced Th17 differentiation.

REFERENCES


1. Glass CK, Saijo K, Winner B, Marchetto MC, Gage FH. Mechanisms underlying inflammation in neurodegeneration. Cell. 2010;140:918–34.

2. Medzhitov R. Inflammation 2010: New adventures of an old flame. Cell. 2010;140:771–6.

3. Grivennikov SI, Greten FR, Karin M. Immunity, inflammation, and cancer. Cell. 2010;140:883–99.

4. Youm Y-H, Grant RW, McCabe LR, Albarado DC, Nguyen KY, Ravussin A, Pistell P, Newman S, Carter R, et al. Canonical Nlrp3 inflammasome links systemic low-grade inflammation to functional decline in aging. Cell Metab. 2013;18:519–32.

5. Bettelli E, Carrier Y, Gao W, Korn T, Strom TB, Oukka M, Weiner HL, Kuchroo VK. Reciprocal developmental pathways for the generation of pathogenic effector TH17 and regulatory T cells. Nature. 2006;441:235–8.

6. Sherman E, Barr V, Samelson LE. Super-resolution characterization of TCR-dependent signaling clusters. Immunol Rev. 2013;251:21–35.

7. Veldhoen M, Hocking RJ, Atkins CJ, Locksley RM, Stockinger B. TGFbeta in the context of an inflammatory cytokine milieu supports de novo differentiation of IL-17-producing T cells. Immunity. 2006;24:179–89.

8. Yang XO, Panopoulos AD, Nurieva R, Chang SH, Wang D, Watowich SS, Dong C. STAT3 regulates cytokine-mediated generation of inflammatory helper T cells. J Biol Chem. 2007;282:9358–63.

9. Tesmer LA, Lundy SK, Sarkar S, Fox DA. Th17 cells in human disease. Immunol Rev. 2008;223:87–113.

10. Witowski J, Pawlaczyk K, Breborowicz A, Scheuren A, Kuzlan-Pawlaczyk M, Wisniewska J, Polubinska A, Friess H, Gahl GM, et al. IL-17 stimulates intraperitoneal neutrophil infiltration through the release of GRO alpha chemokine from mesothelial cells. J Immunol. 2000;165:5814–21.

11. Sonnenberg GF, Fouser LA, Artis D. Border patrol: regulation of immunity, inflammation and tissue homeostasis at barrier surfaces by IL-22. Nat Immunol. 2011;12:383–90.

12. Zheng Y, Valdez PA, Danilenko DM, Hu Y, Sa SM, Gong Q, Abbas AR, Modrusan Z, Ghilardi N, et al. Interleukin-22 mediates early host defense against attaching and effacing bacterial pathogens. Nat Med. 2008;14:282–9.

13. Sugimoto K, Ogawa A, Mizoguchi E, Shimomura Y, Andoh A, Bhan AK, Blumberg RS, Xavier RJ, Mizoguchi A. IL-22 ameliorates intestinal inflammation in a mouse model of ulcerative colitis. J Clin Invest. 2008;118:534–44.

14. Liang SC, Tan X-Y, Luxenberg DP, Karim R, Dunussi-Joannopoulos K, Collins M, Fouser LA. Interleukin (IL)-22 and IL-17 are coexpressed by Th17 cells and cooperatively enhance expression of antimicrobial peptides. J Exp Med. 2006;203:2271–9.

15. Chalaris A, Garbers C, Rabe B, Rose-John S, Scheller J. The soluble interleukin 6 receptor: generation and role in inflammation and cancer. Eur J Cell Biol. 2011;90:484–94.

16. Neurath MF, Finotto S. IL-6 signaling in autoimmunity, chronic inflammation and inflammation-associated cancer. Cytokine Growth Factor Rev. 2011;22:83–9.

17. Silver JS, Hunter CA. gp130 at the nexus of inflammation, autoimmunity, and cancer. J Leukoc Biol. 2010;88:1145–56.

18. Rabe B, Chalaris A, May U, Waetzig GH, Seegert D, Williams AS, Jones SA, Rose-John S, Scheller J. Transgenic blockade of interleukin 6 transsignaling abrogates inflammation. Blood. 2008;111:1021–8.

19. Finotto S, Eigenbrod T, Karwot R, Boross I, Doganci A, Ito H, Nishimoto N, Yoshizaki K, Kishimoto T, et al. Local blockade of IL-6R signaling induces lung CD4+ T cell apoptosis in a murine model of asthma via regulatory T cells. Int Immunol. 2007;19:685–93.

20. Jones GW, McLoughlin RM, Hammond VJ, Parker CR, Williams JD, Malhotra R, Scheller J, Williams AS, Rose-John S, et al. Loss of CD4+ T cell IL-6R expression during inflammation underlines a role for IL-6 trans signaling in the local maintenance of Th17 cells. J Immunol. 2010;184:2130–9.

21. Kang JX. Fat-1 transgenic mice: a new model for omega-3 research. Prostaglandins Leukot Essent Fatty Acids. 2007;77:263–7.

22. Fan Y-Y, Kim W, Callaway E, Smith R, Jia Q, Zhou L, McMurray DN, Chapkin RS. fat-1 transgene expression prevents cell culture-induced loss of membrane n-3 fatty acids in activated CD4+ T-cells. Prostaglandins Leukot Essent Fatty Acids. 2008;79:209–14.

23. Monk JM, Jia Q, Callaway E, Weeks B, Alaniz RC, McMurray DN, Chapkin RS. Th17 cell accumulation is decreased during chronic experimental colitis by (n-3) PUFA in fat-1 mice. J Nutr. 2012;142:117–24.

24. Itariu BK, Zeyda M, Hochbrugger EE, Neuhofer A, Prager G, Schindler K, Bohdjalian A, Mascher D, Vangala S, et al. Long-chain n-3 PUFAs reduce adipose tissue and systemic inflammation in severely obese nondiabetic patients: a randomized controlled trial. Am J Clin Nutr. 2012;96:1137–49.

25. Spencer M, Finlin BS, Unal R, Zhu B, Morris AJ, Shipp LR, Lee J, Walton RG, Adu A, et al. Omega-3 fatty acids reduce adipose tissue macrophages in human subjects with insulin resistance. Diabetes. 2013;62:1709–17.

26. Virtanen JK, Nyantika AN, Kauhanen J, Voutilainen S, Tuomainen T-P. Serum long-chain n-3 polyunsaturated fatty acids, methylmercury and blood pressure in an older population. Hypertens Res. 2012;35:1000–4.

27. Lev EI, Solodky A, Harel N, Mager A, Brosh D, Assali A, Roller M, Battler A, Kleiman NS, Kornowski R. Treatment of aspirin-resistant patients with omega-3 fatty acids versus aspirin dose escalation. J Am Coll Cardiol. 2010;55:114–21.

28. Gebauer SK, Psota TL, Harris WS, Kris-Etherton PM. n−3 Fatty acid dietary recommendations and food sources to achieve essentiality and cardiovascular benefits. Am J Clin Nutr. 2006;83:S1526–1535S.

29. Hibbeln JR, Nieminen LRG, Blasbalg TL, Riggs JA, Lands WEM. Healthy intakes of n-3 and n-6 fatty acids: estimations considering worldwide diversity. Am J Clin Nutr. 2006;83:1483S–1493S.

30. Simopoulos AP. Omega-3 fatty acids in inflammation and autoimmune diseases. J Am Coll Nutr. 2002;21:495–505.

31. Berbert AA, Kondo CRM, Almendra CL, Matsuo T, Dichi I. Supplementation of fish oil and olive oil in patients with rheumatoid arthritis. Nutrition. 2005;21:131–6.

32. Adam O, Beringer C, Kless T, Lemmen C, Adam A, Wiseman M, Adam P, Klimmek R, Forth W. Anti-inflammatory effects of a low arachidonic acid diet and fish oil in patients with rheumatoid arthritis. Rheumatol Int. 2003;23:27–36.

33. Almallah YZ, Richardson S, O'Hanrahan T, Mowat NA, Brunt PW, Sinclair TS, Ewen S, Heys SD, Eremin O. Distal procto-colitis, natural cytotoxicity, and essential fatty acids. Am J Gastroenterol. 1998;93:804–9.

34. Greenfield SM, Green AT, Teare JP, Jenkins AP, Punchard NA, Ainley CC, Thompson RP. A randomized controlled study of evening primrose oil and fish oil in ulcerative colitis. Aliment Pharmacol Ther. 1993;7:159–66.

35. Remans PHJ, Sont JK, Wagenaar LW, Wouters-Wesseling W, Zuijderduin WM, Jongma A, Breedveld FC, Van Laar JM. Nutrient supplementation with polyunsaturated fatty acids and micronutrients in rheumatoid arthritis: clinical and biochemical effects. Eur J Clin Nutr. 2004;58:839–45.

36. Hodge L, Salome CM, Hughes JM, Liu-Brennan D, Rimmer J, Allman M, Pang D, Armour C, Woolcock AJ. Effect of dietary intake of omega-3 and omega-6 fatty acids on severity of asthma in children. Eur Respir J. 1998;11:361–5.

37. Walker CG, Browning LM, Mander AP, Madden J, West AL, Calder PC, Jebb SA. Age and sex differences in the incorporation of EPA and DHA into plasma fractions, cells and adipose tissue in humans. Br J Nutr. 2014;111:679–89.

38. Rees D, Miles EA, Banerjee T, Wells SJ, Roynette CE, Wahle KW, Calder PC. Dose-related effects of eicosapentaenoic acid on innate immune function in healthy humans: a comparison of young and older men. Am J Clin Nutr. 2006;83:331–42.

39. Turner D, Shah PS, Steinhart AH, Zlotkin S, Griffiths AM. Maintenance of remission in inflammatory bowel disease using omega-3 fatty acids (fish oil): a systematic review and meta-analyses. Inflamm Bowel Dis. 2011;17:336–45.

40. Bilal S, Haworth O, Wu L, Weylandt KH, Levy BD, Kang JX. Fat-1 transgenic mice with elevated omega-3 fatty acids are protected from allergic airway responses. Biochim Biophys Acta. 2011;1812:1164–9.

41. Monk JM, Hou TY, Turk HF, Weeks B, Wu C, McMurray DN, Chapkin RS. Dietary n-3 polyunsaturated fatty acids (PUFA) decrease obesity-associated Th17 cell-mediated inflammation during colitis. PloS One. 2012;7:e49739.

42. Todoric J, Löffler M, Huber J, Bilban M, Reimers M, Kadl A, Zeyda M, Waldhäusl W, Stulnig TM. Adipose tissue inflammation induced by high-fat diet in obese diabetic mice is prevented by n-3 polyunsaturated fatty acids. Diabetologia. 2006;49:2109–19.

43. Kim W, Fan Y-Y, Barhoumi R, Smith R, McMurray DN, Chapkin RS. n-3 polyunsaturated fatty acids suppress the localization and activation of signaling proteins at the immunological synapse in murine CD4+ T cells by affecting Lipid raft formation. J Immunol. 2008;181:6236–43.

44. Kim W, Khan NA, McMurray DN, Prior IA, Wang N, Chapkin RS. Regulatory activity of polyunsaturated fatty acids in T-cell signaling. Prog Lipid Res. 2010;49:250–61.

45. Kim W, Fan Y-Y, Smith R, Patil B, Jayaprakasha GK, McMurray DN, Chapkin RS. Dietary curcumin and limonin suppress CD4+ T-cell proliferation and interleukin-2 production in mice. J Nutr. 2009;139:1042–8.

46. Faber J, Berkhout M, Vos AP, Sijben JWC, Calder PC, Garssen J, van Helvoort A. Supplementation with a fish oil-enriched, high-protein medical food leads to rapid incorporation of EPA into white blood cells and modulates immune responses within one week in healthy men and women. J Nutr. 2011;141:964–70.

47. Calder PC. n-3 fatty acids, inflammation and immunity: new mechanisms to explain old actions. Proc Nutr Soc. 2013;72:326–36.

48. Bagga D, Wang L, Farias-Eisner R, Glaspy JA, Reddy ST. Differential effects of prostaglandin derived from omega-6 and omega-3 polyunsaturated fatty acids on COX-2 expression and IL-6 secretion. Proc Natl Acad Sci U S A. 2003;100:1751–6.

49. Nauroth JM, Liu YC, Elswyk MV, Bell R, Hall EB, Chung G, Arterburn LM. Docosahexaenoic acid (DHA) and docosapentaenoic acid (DPAn-6) algal oils reduce inflammatory mediators in human peripheral mononuclear cells in vitro and paw edema in vivo. Lipids. 2010;45:375–84.

50. Mas E, Croft KD, Zahra P, Barden A, Mori TA. Resolvins D1, D2, and other mediators of self-limited resolution of inflammation in human blood following n-3 fatty acid supplementation. Clin Chem. 2012;58:1476–84.

51. Zhao Y, Joshi-Barve S, Barve S, Chen LH. Eicosapentaenoic acid prevents LPS-induced TNF-alpha expression by preventing NF-kappaB activation. J Am Coll Nutr. 2004;23:71–8.

52. Sperling RI, Benincaso AI, Knoell CT, Larkin JK, Austen KF, Robinson DR. Dietary omega-3 polyunsaturated fatty acids inhibit phosphoinositide formation and chemotaxis in neutrophils. J Clin Invest. 1993;91:651–60.

53. Thies F, Nebe-von-Caron G, Powell JR, Yaqoob P, Newsholme EA, Calder PC. Dietary supplementation with γ-linolenic acid or fish oil decreases T lymphocyte proliferation in healthy older humans. J Nutr. 2001;131:1918–27.

54. Zhang P, Kim W, Zhou L, Wang N, Ly LH, McMurray DN, Chapkin RS. Dietary fish oil inhibits antigen-specific murine Th1 cell development by suppression of clonal expansion. J Nutr. 2006;136:2391–8.

55. Monk JM, Hou TY, Turk HF, McMurray DN, Chapkin RS. n3 PUFAs reduce mouse CD4+ T-cell ex vivo polarization into Th17 cells. J Nutr. 2013;143:1501–8.

56. Arrington JL, McMurray DN, Switzer KC, Fan YY, Chapkin RS. Docosahexaenoic acid suppresses function of the CD28 costimulatory membrane receptor in primary murine and Jurkat T cells. J Nutr. 2001;131:1147–53.

57. Jolly CA, McMurray DN, Chapkin RS. Effect of dietary n-3 fatty acids on interleukin-2 and interleukin-2 receptor alpha expression in activated murine lymphocytes. Prostaglandins Leukot Essent Fatty Acids. 1998;58:289–93.

58. Betz UA, Müller W. Regulated expression of gp130 and IL-6 receptor alpha chain in T cell maturation and activation. Int Immunol. 1998;10:1175–84.

59. Briso EM, Dienz O, Rincon M. Cutting edge: soluble IL-6R is produced by IL-6R ectodomain shedding in activated CD4 T cells. J Immunol. 2008;180:7102–6.

60. Mihara M, Hashizume M, Yoshida H, Suzuki M, Shiina M. IL-6/IL-6 receptor system and its role in physiological and pathological conditions. Clin Sci. 2012;122:143–59.

61. Chalaris A, Rabe B, Paliga K, Lange H, Laskay T, Fielding CA, Jones SA, Rose-John S, Scheller J. Apoptosis is a natural stimulus of IL6R shedding and contributes to the proinflammatory trans-signaling function of neutrophils. Blood. 2007;110:1748–55.

62. Classen-Linke I, Müller-Newen G, Heinrich PC, Beier HM, von Rango U. The cytokine receptor gp130 and its soluble form are under hormonal control in human endometrium and decidua. Mol Hum Reprod. 2004;10:495–504.

63. Kwiatek JM, Owen DM, Abu-Siniyeh A, Yan P, Loew LM, Gaus K. Characterization of a new series of fluorescent probes for imaging membrane order. PLoS ONE. 2013;8:e52960.

64. Owen DM, Magenau A, Williamson D, Gaus K. The lipid raft hypothesis revisited – new insights on raft composition and function from super-resolution fluorescence microscopy. BioEssays. 2012;34:739–47.

65. Lingwood D, Simons K. Lipid rafts as a membrane-organizing principle. Science. 2010;327:46–50.

66. Bi K, Tanaka Y, Coudronniere N, Sugie K, Hong S, van Stipdonk MJB, Altman A. Antigen-induced translocation of PKC-θ to membrane rafts is required for T cell activation. Nat Immunol. 2001;2:556–63.

67. Matthews V, Schuster B, Schütze S, Bussmeyer I, Ludwig A, Hundhausen C, Sadowski T, Saftig P, Hartmann D, et al. Cellular cholesterol depletion triggers shedding of the human interleukin-6 receptor by ADAM10 and ADAM17 (TACE). J Biol Chem. 2003;278:38829–39.

68. Stillwell W, Shaikh SR, Zerouga M, Siddiqui R, Wassall SR. Docosahexaenoic acid affects cell signaling by altering lipid rafts. Reprod Nutr Dev. 2005;45:559–79.

69. Turk HF, Chapkin RS. Membrane lipid raft organization is uniquely modified by n-3 polyunsaturated fatty acids. Prostaglandins Leukot Essent Fatty Acids. 2013;88:43–7.

70. Zhu Y, Gumlaw N, Karman J, Zhao H, Zhang J, Jiang J-L, Maniatis P, Edling A, Chuang W-L, et al. Lowering glycosphingolipid levels in CD4+ T cells attenuates T cell receptor signaling, cytokine production, and differentiation to the Th17 lineage. J Biol Chem. 2011;286:14787–94.

71. Buk DM, Waibel M, Braig C, Martens AS, Heinrich PC, Graeve L. Polarity and lipid raft association of the components of the ciliary neurotrophic factor receptor complex in Madin-Darby canine kidney cells. J Cell Sci. 2004;117:2063–75.

72. Yanagisawa M, Nakamura K, Taga T. Roles of lipid rafts in integrin-dependent adhesion and gp130 signalling pathway in mouse embryonic neural precursor cells. Genes Cells. 2004;9:801–9.

73. Jia Q, Lupton JR, Smith R, Weeks BR, Callaway E, Davidson LA, Kim W, Fan Y-Y, Yang P, et al. Reduced colitis-associated colon cancer in fat-1 (n-3 fatty acid desaturase) transgenic mice. Cancer Res. 2008;68:3985–91.

74. Dong L, Watanabe K, Itoh M, Huan C-R, Tong X-P, Nakamura T, Miki M, Iwao H, Nakajima A, et al. CD4+ T-cell dysfunctions through the impaired lipid rafts ameliorate concanavalin A-induced hepatitis in sphingomyelin synthase 1-knockout mice. Int Immunol. 2012;24:327–37.

75. Adler J, Parmryd I. Quantifying colocalization by correlation: the Pearson correlation coefficient is superior to the Mander's overlap coefficient. Cytom A. 2010;77:733–42.

76. Galland L. Diet and inflammation. Nutr Clin Pract. 2010;25:634–40.

77. Bulló M, Casas-Agustench P, Amigó-Correig P, Aranceta J, Salas-Salvadó J. Inflammation, obesity and comorbidities: the role of diet. Public Health Nutr. 2007;10:1164–72.

78. Miles EA, Calder PC. Influence of marine n-3 polyunsaturated fatty acids on immune function and a systematic review of their effects on clinical outcomes in rheumatoid arthritis. Br J Nutr. 2012;107 Suppl 2:S171–184.

79. Hong S, Gronert K, Devchand PR, Moussignac R-L, Serhan CN. Novel docosatrienes and 17S-resolvins generated from docosahexaenoic acid in murine brain, human blood, and glial cells. Autacoids in anti-inflammation. J Biol Chem. 2003;278:14677–87.

80. Galet C, Gollapudi K, Stepanian S, Byrd JB, Henning SM, Grogan T, Elashoff D, Heber D, Said J, et al. Effect of a low-fat fish oil diet on proinflammatory eicosanoids and cell-cycle progression score in men undergoing radical prostatectomy. Cancer Prev Res. 2014;7:97–104.

81. Kelley DS, Taylor PC, Nelson GJ, Schmidt PC, Ferretti A, Erickson KL, Yu R, Chandra RK, Mackey BE. Docosahexaenoic acid ingestion inhibits natural killer cell activity and production of inflammatory mediators in young healthy men. Lipids. 1999;34:317–24.

82. Yang P, Chan D, Felix E, Cartwright C, Menter DG, Madden T, Klein RD, Fischer SM, Newman RA. Formation and antiproliferative effect of prostaglandin E(3) from eicosapentaenoic acid in human lung cancer cells. J Lipid Res. 2004;45:1030–9.

83. Stanke-Labesque F, Molière P, Bessard J, Laville M, Véricel E, Lagarde M. Effect of dietary supplementation with increasing doses of docosahexaenoic acid on neutrophil lipid composition and leukotriene production in human healthy volunteers. Br J Nutr. 2008;100:829–33.

84. Barros KV, Cassulino AP, Schalch L, Munhoz EDV, Manetta JA, Calder PC, Silveira VLF. Pharmaconutrition: acute fatty acid modulation of circulating cytokines in elderly patients in the ICU. J Parenter Enteral Nutr. 2013;

85. Meydani SN, Endres S, Woods MM, Goldin BR, Soo C, Morrill-Labrode A, Dinarello CA, Gorbach SL. Oral (n-3) fatty acid supplementation suppresses cytokine production and lymphocyte proliferation: comparison between young and older women. J Nutr. 1991;121:547–55.

86. Trebble T, Arden NK, Stroud MA, Wootton SA, Burdge GC, Miles EA, Ballinger AB, Thompson RL, Calder PC. Inhibition of tumour necrosis factor-alpha and interleukin 6 production by mononuclear cells following dietary fish-oil supplementation in healthy men and response to antioxidant co-supplementation. Br J Nutr. 2003;90:405–12.

87. Kolahi S, Ghorbanihaghjo A, Alizadeh S, Rashtchizadeh N, Argani H, Khabazzi A-R, Hajialilo M, Bahreini E. Fish oil supplementation decreases serum soluble receptor activator of nuclear factor-kappa B ligand/osteoprotegerin ratio in female patients with rheumatoid arthritis. Clin Biochem. 2010;43:576–80.

88. Luostarinen R, Saldeen T. Dietary fish oil decreases superoxide generation by human neutrophils: relation to cyclooxygenase pathway and lysosomal enzyme release. Prostaglandins Leukot Essent Fatty Acids. 1996;55:167–72.

89. Hughes DA, Pinder AC. n-3 polyunsaturated fatty acids inhibit the antigen-presenting function of human monocytes. Am J Clin Nutr. 2000;71:357S–60S.

90. Korn T, Bettelli E, Oukka M, Kuchroo VK. IL-17 and Th17 Cells. Annu Rev Immunol. 2009;27:485–517.

91. Michalek RD, Gerriets VA, Jacobs SR, Macintyre AN, MacIver NJ, Mason EF, Sullivan SA, Nichols AG, Rathmell JC. Cutting edge: distinct glycolytic and lipid oxidative metabolic programs are essential for effector and regulatory CD4+ T cell subsets. J Immunol. 2011;186:3299–303.

92. Nishihara M, Ogura H, Ueda N, Tsuruoka M, Kitabayashi C, Tsuji F, Aono H, Ishihara K, Huseby E, et al. IL-6–gp130–STAT3 in T cells directs the development of IL-17+ Th with a minimum effect on that of Treg in the steady state. Int Immunol. 2007;19:695–702.

93. Jadidi-Niaragh F, Mirshafiey A. Th17 cell, the new player of neuroinflammatory process in multiple sclerosis. Scand J Immunol. 2011;74:1–13.

94. Eastaff-Leung N, Mabarrack N, Barbour A, Cummins A, Barry S. Foxp3+ regulatory T cells, Th17 effector cells, and cytokine environment in inflammatory bowel disease. J Clin Immunol. 2010;30:80–9.

95. Huber S, Gagliani N, Flavell RA. Life, death, and miracles: Th17 cells in the intestine. Eur J Immunol. 2012;42:2238–45.

96. Van Hamburg JP, Corneth OBJ, Paulissen SMJ, Davelaar N, Asmawidjaja PS, Mus AMC, Lubberts E. IL-17/Th17 mediated synovial inflammation is IL-22 independent. Ann Rheum Dis. 2013;72:1700–7.

97. Samoilova EB, Horton JL, Hilliard B, Liu T-ST, Chen Y. IL-6-deficient mice are resistant to experimental autoimmune encephalomyelitis: roles of IL-6 in the activation and differentiation of autoreactive T cells. J Immunol. 1998;161:6480–6.

98. Zhang P, Smith R, Chapkin RS, McMurray DN. Dietary (n-3) polyunsaturated fatty acids modulate murine Th1/Th2 balance toward the Th2 pole by suppression of Th1 development. J Nutr. 2005;135:1745–51.

99. Sostres C, Gargallo CJ, Arroyo MT, Lanas A. Adverse effects of non-steroidal anti-inflammatory drugs (NSAIDs, aspirin and coxibs) on upper gastrointestinal tract. Best Pract Res Clin Gastroenterol. 2010;24:121–32.

100. Fan Y-Y, Kim W, Callaway E, Smith R, Jia Q, Zhou L, McMurray DN, Chapkin RS. fat-1 transgene expression prevents cell culture-induced loss of membrane n-3 fatty acids in activated CD4+ T-cells. Prostaglandins Leukot Essent Fatty Acids. 2008;79:209–14.

101. Reagan-Shaw S, Nihal M, Ahmad N. Dose translation from animal to human studies revisited. FASEB J. 2008;22:659–61.

102. Kim W, McMurray DN, Chapkin RS. n-3 polyunsaturated fatty acids--physiological relevance of dose. Prostaglandins Leukot Essent Fatty Acids. 2010;82:155–8.

103. Feskens EJ, Kromhout D. Epidemiologic studies on Eskimos and fish intake. Ann N Y Acad Sci. 1993;683:9–15.

104. Souwer Y, Wit J de, Muller FJM, Bos HK, Jorritsma T, Kapsenberg ML, Jong EC de, Ham SM van. Response: priming of human naive CD4+ T cells via CD5 costimulation requires IL-6 for optimal Th17 development. Blood. 2012;119:4812–3.

105. Ivanov II, McKenzie BS, Zhou L, Tadokoro CE, Lepelley A, Lafaille JJ, Cua DJ, Littman DR. The orphan nuclear receptor RORgammat directs the differentiation program of proinflammatory IL-17+ T helper cells. Cell. 2006;126:1121–33.

106. Serada S, Fujimoto M, Mihara M, Koike N, Ohsugi Y, Nomura S, Yoshida H, Nishikawa T, Terabe F, et al. IL-6 blockade inhibits the induction of myelin antigen-specific Th17 cells and Th1 cells in experimental autoimmune encephalomyelitis. Proc Natl Acad Sci USA. 2008;105(26):9041-6

107. Liu X, Lee YS, Yu C-R, Egwuagu CE. Loss of STAT3 in CD4+ T cells prevents development of experimental autoimmune diseases. J Immunol. 2008;180:6070–6.

108. Raza Shaikh S. Diet-induced docosahexaenoic acid non-raft domains and lymphocyte function. Prostaglandins Leukot Essent Fat Acids. 2010;82:159–64.

109. Shaikh SR, Dumaual AC, Jenski LJ, Stillwell W. Lipid phase separation in phospholipid bilayers and monolayers modeling the plasma membrane. Biochim Biophys Acta. 2001;1512:317–28.

110. Shaikh SR, Rockett BD, Salameh M, Carraway K. Docosahexaenoic acid modifies the clustering and size of lipid rafts and the lateral organization and surface expression of MHC class I of EL4 cells. J Nutr. 2009;139:1632–9.

111. Xu L, Kitani A, Fuss I, Strober W. Cutting edge: regulatory T cells induce CD4+CD25-Foxp3- T cells or are self-induced to become Th17 cells in the absence of exogenous TGF-beta. J Immunol. 2007;178:6725–9.

112. Calder PC. n−3 Polyunsaturated fatty acids, inflammation, and inflammatory diseases. Am J Clin Nutr. 2006;83:S1505–1519S.

113. Coxib and Traditional NSAID Trialists' (CNT) Collaboration. Vascular and upper gastrointestinal effects of non-steroidal anti-inflammatory drugs: meta-analyses of individual participant data from randomised trials. The Lancet. 2013;382:769–79.

114. Van Everdingen AA, Jacobs JWG, Siewertsz van Reesema DR, Bijlsma JWJ. Low-dose prednisone therapy for patients with early active rheumatoid arthritis: clinical efficacy, disease-modifying properties, and side effects: a randomized, double-blind, placebo-controlled clinical trial. Ann Intern Med. 2002;136:1–12.

# APPENDIX A

## ISOLATION OF $CD4^+$ T CELLS USING MILTENYI BEAD/COLUMN

**Reagents:**
Scissors and forceps for animal surgery
70 μm Cell Strainer (BD 352350)
30 μm MACS pre-separation filter (Miltenyi 08-771-2)
MACS separation LS columns (Miltenyi 130-042-401)
5 mL Syringes → just need the plunger part (BD 309646)
QuadroMACS Separation Unit (Miltenyi 130-090-976)
100 mm Petri dish (BD 351029)
Auto MACS Running Buffer (Miltenyi 130-091-221)
CD4 (L3T4) Microbeads, mouse (Miltenyi 130-049-201)
PBS (Gibco, 14190)
RPMI (Irvine Scientific, 9159)
Heat-inactivated FBS (Irvine Scientific, 300320439)
Glutamax (Gibco, 35050-061)
Penicillin-Streptomycin (Gibco, 15140-148)
Isoton Fluid (Beckman Coulter)
Specialty clear pipette tips (Fisher Scientific, 21-375-12)

**Procedure:**

1. Aliquot 50ml MACS buffer and RPMI media (if needed) and keep on ice before beginning.
2. Remove the spleen from a mouse and place the spleen in 15 mL conical tube containing 3 mL of MACS buffer.
    a. Remove as much fat as possible from the spleen.
3. Place 70 μm cell strainer inside a 100 mm Petri dish and wet the membrane by adding 5 mL of MACS buffer.
4. Place a 30 μm MACS pre-separation filter on top of a new 15 mL conical tube. Wet the filter with 2 mL MACS buffer.
5. Transfer the spleen with the 3 mL MACS buffer onto the cell strainer and use the plunger to mesh (gently push, not grind) the tissue inside the Petri dish.
    a. Keep the tissue wet at all times.
    b. Continue until only connective tissue is left on the membrane.
    c. Use Petri dish or else cells will adhere to the plate.
6. Wash the plate with the MACS buffer in the Petri dish.
7. Remove the cell strainer and transfer the 8 mL of buffer containing cells onto the 30 μm MACS pre-separation filter slowly (small volume at a time to prevent clogging).

8. Wash the cell strainer by washing it inside the Petri dish with 5 mL of MACS buffer. Wash the Petri dish again, and apply to the 30 μm MACS pre-separation filter.
9. Remove the filter, close the lid, and gently invert the tube. Take 20 μL and count using Coulter counter (4 μm cut off).
10. Centrifuge cell suspension at 300 x g for 10 min and use a plastic tip to aspirate off the supernatant.
11. Tap the bottom of the tube to loosen the pellet and then add 90 μL/$10^7$ total cells of MACS buffer to get a good suspension.
    a. Know the amount of cells by using the Coulter counter. The approximate volume of cells is 13.5 mL (some is lost in wetting the membranes).
    b. Can only load up to 2 x $10^9$ total cells ($10^8$ labeled cells) per LS column.
    c. Make sure to record the starting cell numbers for calculating yields.
12. Add 10 μL/$10^7$ total cells of CD4 (L3T4) microbeads directly into the suspension.
13. Mix well by pipetting and incubate for 15 min at 4 °C (use refrigerator, do not shake).
14. Wash cells by filling up the 15 mL conical tube with cold MACS buffer. Mix by inversion, centrifuge at 300 g for 10 min, and then use a plastic tip to aspirate off the supernatant.
15. Tap the bottom of the tube to loosen the pellet and then add 500 μL/$10^8$ total cells of MACS buffer to get a good suspension.
16. Snap the LS column into the QuadroMACS Separator. Orient the column so that the smooth side goes into the separator. Place a basin under the column for waste. Pre-wet the LS column with 500 μL of cold MACS buffer. Let the buffer slowly drip through.
17. Apply the cell suspension onto the column.
    a. Can collect the flow-through to collect $CD4^-$ cell population.
18. To rinse column, first wash the tube from Step 16 with 9 mL of cold MACS buffer and then apply 3 mL to the column. Allow the buffer to run through the column before applying an additional 3 mL twice.
    a. This washes the unlabeled cells through the column.
19. Remove the columns from the separator and place it on 15 mL conical tube for collection.
20. Pipette 5 mL of cold MACS buffer onto the column. Immediately flush out by applying the plunger supplied with the column. Push the plunger into the column all the way.
    a. This fraction contains the magnetically labeled cells.
21. Fill the tube with an additional 5 mL of cold MACS buffer. Invert to wash well.
22. Centrifuge the elution at 300 g for 10 min. Aspirate off the supernatant.
23. Fill the tube with 10 mL of ice cold PBS. Wash by inversion. Take 20 μL of the suspension and count using the Coulter Counter. Use trypan blue and a hemacytometer to measure viability as well.

24. Centrifuge the elution at 300 g for 10 min. Aspirate off the supernatant. Proceed to downstream applications.

*Notes:*

- All the steps are performed in cell culture hood except the removal of the spleen from the mouse.
- Store and use MACS buffer on ice, but perform rest of procedure at room temperature.
- Pour out 50 mL of MACS buffer into a conical tube so that the stock MACS does not get contaminated.
- Remember to prepare the Isoton Fluid the day before (dispense 10 mL into the cuvette and let sit to get rid of air bubbles).

APPENDIX B

FLOW CYTOMETRY SURFACE STAINING PROTOCOL

**Purpose: To measure surface expression of membrane bound receptors (IL-6R and gp130) in mouse $CD4^+$ T cells.**

**Reagents:**
RPMI (Irvine Scientific, 9159)
Heat-inactivated FBS (Irvine Scientific, 300320439)
Glutamax (Gibco, 35050-061)
Pen-strep (Gibco, 15140-148)
Flow cytometry staining buffer (eBioscience #00-4222-26)
96 well round bottom plate (BD Falcon #353077)
Anti-IL-6R (BD #554462) or anti-gp130 (BD Pharmingen 554462)
FC Block (eBioscience 14-0161-86)
Flow cytometry micro tubes (BioRad #223-9391)

**Procedure:**

1. Make complete RPMI consisting of 1L RPMI, 100 mL heat-inactivated FBS, 11 mL Glutamax and 11 mL Pen-strep.
2. Isolate $CD4^+$ T cells from mouse spleen according to Miltenyi protocol.
3. Resuspend cells in complete RPMI to a final concentration of 1 million viable cells per mL.
4. Seed 200 µl of cells in complete RPMI into each well of a 96-well round bottom plate.
5. Centrifuge the plates at 350xg for 2 minutes at 4˚C
6. Aspirate the top ¾ of the fluid with an 8 channel pipette leaving approximately 50 µl in each well.
7. Replace the lid back on the plate and gently tap all four sides of the plate multiple times to disrupt the pellet (don't spill fluid onto lid).
8. Add a maximum of 180 µl of flow cytometry staining buffer to each well.
9. Centrifuge the plates at 350xg for 2 minutes at 4˚C.
10. Aspirate the top ¾ of the fluid with an 8 channel pipette leaving approximately 50 µl in each well and gently tap the plate to disrupt the pellet.
11. Add 50 µl staining buffer to each well.
12. Add 2 ul of FC block to each well and incubate at 4ºC for 15 minutes.
13. Add flow antibody (need to optimize antibody mass first) to stained wells and incubate on ice protected from light for 30 minutes.
    -0.5 µg each of anti-IL-6R and anti-gp130
14. Wash by adding 100 µl of staining buffer and centrifuge at 350xg for 2 minutes at 4˚C.

15. Aspirate the top ¾ of the fluid with an 8 channel pipette leaving approximately 50 µl in each well and gently tap the plate to disrupt the pellet.
16. Add 180 µl of staining buffer and centrifuge at 350xg for 2 minutes at 4˚C.
17. Aspirate the top ¾ of the fluid with an 8 channel pipette leaving approximately 50 µl in each well and gently tap the plate to disrupt the pellet.
18. Transfer the contents of each well to a flow micro tube and keep on ice protected from light.
19. Run all samples on the Accuri right away

**Note: How to use Quantibrite (BD) Beads**

1. Keep beads in foil pouches stored at 2°-8°C before use.
2. Reconstitute beads in buffer (PBS with 0.5% BSA plus a sprinkle of sodium azide-use as little as possible for this small volume) before use. Beads are stable for 24 hours but make as close to use as possible.
3. Vortex quickly and run on Accuri with the same settings as samples (in this case run on slow) and collect 10,000 events.
4. Parameters should be SSC-H (y-axis) vs FSC-H (x-axis).
5. Gate around the bead singlets (see the technical data sheet for assistance)
6. Create a histogram with count on the y axis and FL2 on the x axis. Adjust the markers around each population (see below figure).

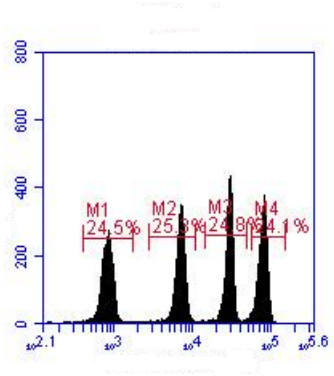


7. Graph the $\log_{10}$ geometric mean for each population against the $\log_{10}$ lot specific PE values (on the box).

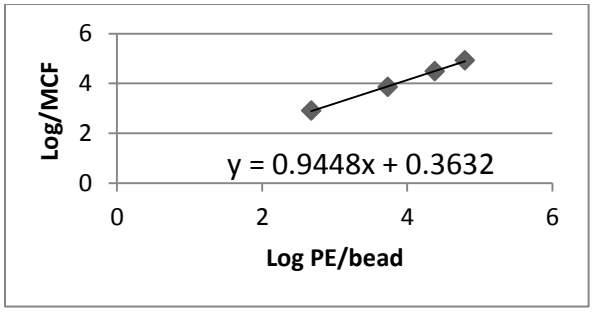


8. Calculate the antibodies bound per cell (x) using the median channel fluorescence for each sample as the ‘y’ in the equation (see technical data sheet for mathematical help)\

APPENDIX C

MEASUREMENT OF ACTIVATION INDUCED CHANGES IN SOLUBLE AND SURFACE IL-6R IN MOUSE $CD4^+$ T CELLS

**Purpose: We have previously shown a decrease in surface expression of IL-6R in *fat-1* mice $CD4^+$ T cells. We aim to determine if this change is due to increased shedding to soluble IL-6R. We will therefore measure surface expression as well as soluble IL-6R at time 0, 24hr, 48hr and 72hr.**

**References:**
R&D Protocol for Mouse IL-6R alpha DuoSet, 15 Plate (#DY1830)

**Reagent:**
96 well round bottom plate (BD Falcon #353077)
Anti-CD3 (BD #553057)
RPMI (Irvine Scientific, 9159)
Heat-inactivated FBS (Irvine Scientific, 300320439)
Glutamax (Gibco, 35050-061)
Pen-strep (Gibco, 15140-148)
TNF-α protease inhibitor (TAPI) (Santa Cruz sc-203410)
DMSO (Sigma D8418)
β-mercaptoethanol (Sigma, M7522)
Anti CD28 (eBioscience #14-0281-86)
Flow Cytometry Staining Buffer (eBioscience #00-4222-26)
Anti-IL-6R (BD #554462)
Fc Block (eBioscience 14-0161-86)
Quantibrite PE Beads (BD 340495)
.

**Procedure:**

1. **THE DAY BEFORE**: Dilute anti-CD3 in sterile PBS to a final concentration of 5μg/ml (1:200 dilution) and coat activated wells overnight at 4˚C. Maintain sterility by not lifting the lids off the plates when outside the hood.

2. **Also the day before:** Make complete RPMI based on recipe below by adding FBS, Glutamax and Pen-strep to a 1L bottle of RPMI.

| | Volume (mL) | % | Stock Concentration | Final Concentration |
|---|---|---|---|---|
| RPMI | 1,000 | 88 | | |

| | | | | |
|---|---|---|---|---|
| Heat-inactivated FBS | 100 | 10 | | |
| Glutamax | 11 | 1 | 200 mM | 2 mM |
| Pen-strep | 11 | 1 | P 10000 U/mL<br>S 10000 µg/mL | P 100 U/mL<br>S 100 µg/mL |

**Day 1**

3. Resuspend 1 mg TAPI in 200 ul (0.22 µm filterered) DMSO to make a 5 mg/mL solution.
4. Make 50 µM β-mercaptoethanol. First dilute 1 µl of the 10 mM stock with 1.43 ml complete RPMI. Then dilute 1:200 with 50 ml complete RPMI and 250 µl 10mM β-mercaptoethanol.
5. Purify mouse splenic $CD4^+$ T cells according to Appendix A Isolation of $CD4^+$ T cells Miltenyi bead/column.
6. Use a 96-well round bottom plate and adjust to 4 million cells per mL in complete RPMI with 50uM 2-mercaptoethanol. Cell counts must be assessed using the hemocytometer and viability is assessed by Trypan blue exclusion.
7. Make two master mixes to add to each well. For each well of activated cells, add 2 µl anti-CD28 (final concentration=5 µg/mL) and 0.9 µl DMSO in 97.1 µl complete RPMI. For each activated well receiving TAPI, add 2 µl anti-CD28 and 0.9 µl TAPI in DMSO in 97.1 µl complete RPMI.
8. Add 100 µl of cells to each well. Add the appropriate master mix (complete RPMI for unstimulated cells). Incubate at 37°C for 48 hours.
9. Centrifuge cells for 5 minutes at 4ºC at 350xg and aspirate 180 µl of supernatant from each well for ELISA analysis (store at -80ºC).
10. Analyze surface expression of IL-6R by flow.

**Soluble receptor ELISA**

**Reagents:**

IL-6R ELISA kit (R&D DY1830)
96 well microplate (high binding) (R&D DY990)
3, 3′,5,5′-Tetramethylbenzidine (TMB) (Biolegend 421501)
Stop Solution-2 N $H_2SO_4$ (Fisher Scientific SA213)

**Procedure:**

**Day Before**

1. Dilute the Capture Antibody to the working concentration in PBS without carrier protein. Stock concentration is 288 g/mL of goat anti-mouse sIL-6R when reconstituted with 1.0 mL of PBS.
2. Dilute to a working concentration of 1.6 g/mL in PBS, without carrier protein (1:180 dilution).

3. Immediately coat a 96-well high binding microplate with 100 µl per well of the diluted Capture Antibody. Seal the plate and incubate overnight at room temperature.

**(Day 1)** 4. Aspirate each well and wash three times with 400 µl wash buffer. Complete removal of liquid at each step is essential for good performance. After the last wash, remove any remaining wash buffer by aspirating or by inverting the plate and blotting it against clean paper towels.

4. Block plates by adding 250 µL of Reagent Diluent to each well. Incubate at room temperature for 1 hour.
5. Repeat the aspiration/wash as in step 4. The plates are now ready for sample addition.
6. Add 100 µL of sample or standards in Reagent Diluent per well. Cover with an adhesive strip and incubate 2 hours at room temperature.
    a. Each vial of standards contains 130 ng/mL of recombinant mouse sIL-6R when reconstituted with 0.5 mL of Reagent Diluent. Allow the standard to sit for a minimum of 15 minutes with gentle agitation prior to making dilutions. A seven point standard curve using 2-fold serial dilutions in Reagent Diluent and a high standard of 3000 pg/mL is recommended.
7. Repeat the aspiration/wash as in step 4.
8. Add 100 µL of the detection antibody, diluted in reagent diluent, to each well. Cover with a new adhesive strip and incubate 2 hours at room temperature.
    a. Detection antibody stock is 36 µg/mL of biotinylated goat anti-mouse sIL-6R when reconstituted with 1.0 mL of reagent diluent.
    b. Dilute to a working concentration of 200 ng/mL in reagent diluent
9. Repeat the aspiration/wash as in step 4.
10. Add 100 µL of the working dilution of Streptavidin-HRP to each well. Cover the plate with aluminum foil to protect form light and incubate for 20 minutes at room temperature.
    a. Streptavidin-HRP consists of 1.0 mL of streptavidin conjugated to horseradish-peroxidase. Dilute to the working concentration specified on the vial label using reagent diluent.
11. Repeat the aspiration/wash as in step 4.
12. Add 100 µL of TMB to each well. Incubate for 20 minutes at room temperature. Avoid placing the plate in direct light.
13. Add 50 µL of Stop Solution to each well. Gently tap the plate to ensure thorough mixing.

    Determine the optical density of each well immediately, using a microplate reader set to 450 nm with wavelength correction at 540 nm.

APPENDIX D

RNA ISOLA FROM $CD4^+$ T CELLS

**Purpose: To extract RNA from $CD4^+$ T cells for PCR analysis of gene expression.**

**Reagents:**
RNAqueous Kit (Ambion AM1914)
DNase (Life Technologies AM 1906)

**Procedure:**

1. Prepare 64% ethanol solution (38.4 mL 100% ethanol (ACS grade or equivalent) to the "Water for 64% Ethanol" bottle.
2. Prepare wash solution #2/3 (64 mL 100% ethanol to "Wash Solution #2/3 Concentrate")
3. Clean bench and pipets with an RNase decontamination solution and change gloves frequently throughout.
4. Follow Appendix A Isolation of $CD4^+$ T cells Miltenyi bead/column
5. Collect cells in an RNase free 1.5 mL tube. Centrifuge at 350 x g for 10 min at 4ºC.
6. Aspirate supernatant and wash cells with 1mL PBS. Centrifuge at 350 x g for 10 min at 4ºC.
7. Aspirate supernatant and add 500 µl lysis/binding solution. Vortex lysate vigorously (may need to sonicate or pass through a 25 g syringe needle) and store at -80 if not isolating RNA that day.
8. For RNA Isolation: Heat an aliquot of elution solution (50 µl per sample) in an RNase-free microcentrifuge tube to 70-80 °C.
9. Reduce viscosity of lysate (by sonication, homogenization or syringe) if necessary (should be ~as viscous as 50% glycerol)
10. If using more than $10^7$ cells, centrifuge for 2-3 minutes at 13,000 rpm in a microcentrifuge to remove debris.
11. Add 500 µl 64% ethanol to lysate and mix gently by pipetting or vortexing.
12. Add lysate/ethanol mix to filter cartridge in a collection tube. Max volume that can be applied is 700 µl.
13. Centrifuge at 13,000 rpm for 30 sec until mixture is through the filter.
14. Discard flow through and repeat once more until entire 1mL goes through filter.
15. Add 700 µl Wash solution 1 to filter cartridge
16. Centrifuge at 13,000 rpm for 30 sec until mixture is through the filter.
17. Discard flow through and add 500 µl Wash solution #2/3.

18. Centrifuge at 13,000 rpm for 30 sec until mixture is through the filter.
19. Discard flow through and add a second 500 µl of Wash solution #2/3.
20. Centrifuge at 13,000 rpm for 30 sec until mixture is through the filter.
21. Discard flow through and centrifuge once more for 1 minute to remove last traces of wash solution.
22. Put filter cartridge into a new collection tube. Add preheated elution solution 50 µl to center of filter and close cap.
23. Recover eluate by centrifugation for 30 seconds at 13,000 x g.
24. Add 5 µl 10X DNase I Buffer and 1 ul DNase I and mix. Incubate at 37ºC for 20-30 minutes.
25. Resuspend DNase inactivation reagent by flicking and vortexing. Add 5 µl DNase inactivation reagent and mix well. Incubate for 2 minutes at room temp, mixing 2-3 times.
26. Centrifuge at 10,000 x g for 1.5 minutes and transfer supernatant (contains RNA) to fresh RNase-free tube.
27. Measure RNA yield and purity by nanodrop and bioanalyzer.

APPENDIX E

IMMUNOFLUORESCENCE IN $CD4^+$ T CELLS

**Purpose: To measure the co-localization of surface proteins (gp130) with lipid rafts in $CD4^+$ T Cells**

**Reagents:**
No. 1.5 Coverglass (Corning, 2935-225)
Lab-Tek II 2-well glass chamber slide (Nalge, 154461)
Anti-CD3 (eBioscience, 16-0031-85)
Anti-CD28 (eBioscience, 14-0281)
Primary Antibody-Rat anti-mouse gp130 (R&D MAB4681)
Secondary Antibody- Alexa 555 goat anti-rat IgG (Invitrogen A21434)
Rat IgG2A Isotype Control (R&D MAB006)
Cholera toxin B-Alexa 488 (Life Technologies V34403)
Coverglass antifade reagent medium (Invitrogen, P36934)
100 mM glycine (Sigma, G7126) in PBS
0.1% (w/v) Poly-L-Lysine solution (Sigma, P8920)
20% PFA in PBS (EMS, 15713-S)
10% Triton X-100 (Fluka, 93443)
Blocking solution-10% Goat Serum (Jackson Laboratory) in PBS-0.22um filtered
RPMI (Irvine Scientific, 9159)
Heat-inactivated FBS (Irvine Scientific, 300320439)
Glutamax (Gibco, 35050-061)
Pen-strep (Gibco, 15140-148)

**Procedures:**
**Day Before**

1. Make complete RPMI according to recipe above. Pre-coat slides (see below). Remember to fill Coulter Counter cups.
2. Precoat chamber slides:
    a. Dilute 10X poly-L-Lysine solution with sterile $H_2O$ to 1X (*0.1% w/v to 0.01% w/v)*
    b. Precoat Lab-Tek II 2-well glass chamber slides with 0.01% poly-L-lysine (*add 2 mL of 0.01% poly-L-Lysine/well for* 30 min *at room temperature. Replace the lids back on while the chamber slides are incubating.)*
3. Aspirate excess solution and sterilize the slides under UV light for 1 hr. Leave the lids off.
4. **If activating with anti-CD3/anti-CD28**: (If not activating, store at RT in a drawer to further protect from light and proceed to step 5).
    a. Dilute anti-CD3 (*stock 1 mg/mL*) 1:1000 and anti-CD28 (*stock 1 mg/mL*) 1:100 in 1X PBS.

b. Add 200 µL of antibodies per chamber slide. For control (unstimulated), add 200 µL of cold 1X PBS per chamber slide.
c. Incubate chamber slides on an orbital shaker (Bellco) (gently) in the 4 °C walk-in cold room at a speed setting of 4, overnight. Replace the lids back on to ensure sterility

5. **Day 1:** wash chamber slides with 1 mL of warm complete RPMI one time.
6. Prewarm the coated chamber slides with 200 µL of warm complete RPMI at 37 °C for 30 or more minutes. Leave in the incubator until seeding.
7. **Isolation of $CD4^+$ T Cells**. Follow Isolation of T cells protocol.
8. After isolation of T cells, re-suspend the $CD4^+$ T cells with warm complete RPMI to get a final concentration of T cells at $5 \times 10^6$ cells/mL in complete RPMI media.
9. Seed 1 mL/well dropwise by adding the cell suspension onto the 200 µL complete media in the well. *This equates to $5 \times 10^6$ cells per well.*
    a. *(If activated) Final anti-CD3 concentration = 0.17 µg/mL (but is actually higher since plated, not suspended).Final anti-CD28 concentration = 1.67 µg/mL (but is actually higher since plated, not suspended).*
10. Incubate at 37 °C for 30 minutes.
11. Make 4% PFA by combining 20% PFA (1:5 dilution) in 1X PBS. Do this in the chemical hood! *Always make PFA fresh (i.e. the same day of experiment).*
12. Wash the cells on the chamber slides with 2 mL PBS 3 times for 2 min each, then immediately fix the cells in 2mL freshly made 4% PFA for 30 min at room temperature. *Do this in the chemical hood!*
13. Rinse the samples with 2mL PBS 2 times for 2 min each, and quench cells with 2mL 100 mM glycine in PBS (37°C) for 2 x 10 min at room temperature (gentle shaking in dark).
    a. *This step is performed to quench aldehyde groups.*
    b. *Do first wash in chemical hood and dump into waste.*
    c. *Make glycine ahead of time and warm in the water bath (37°C) for ~15 minutes. Quench slides on the Bellydancer (gentle shaking) with foil to protect from light.*
14. Wash the chamber slides with 2 mL PBS 2 times for 2 min each, and permeabilize the cells by using 2 mL 0.2% Triton X-100 in PBS for 5 min at room temperature.
    a. *Stock is at 10%, so dilute 1:50 in 1X PBS.*
15. Wash the chamber slides with 2 mL PBS 3 times for 2 min each.
16. Incubate cells in 1 mL blocking solution at room temp (gentle shaking) for 1 hour in a humid chamber. Wash the chamber slides with PBS 3 times for 2 min each.
    *a. Make humid chamber by thoroughly wetting a couple paper towels with PBS and placing at the bottom of a Tupperware container. Place the slide holder on top of the wet paper towels and place a few more wet paper towels on top. Seal tightly with the lid.*

17. Dilute the antibody in the following manner in the dark. To properly resuspend antibody, flick and invert 4 times and centrifuge quickly.

| Antibody | Stock | Dilution | Final |
|---|---|---|---|
| Rat anti-mouse gp130 | 500 µg/mL | 1:100 | 5 µg/mL |
| Rat IgG 2A | 500 µg/mL | 1:100 | 5 µg/mL |

18. Incubate each chamber slide with 300 µL blocking solution + 1° antibody in a humid chamber overnight (gentle shaking). The slides must be protected from light.
19. Wash slides 3 times for 5 minutes with PBS and incubate each chamber slide with 300 µL blocking solution plus 2° antibody per well at room temperature for 2 hrs in a humid chamber. The slides much be protected from light. To properly resuspend antibody, flick and invert 4 times and centrifuge quickly.

| Antibody | Stock | Dilution | Final |
|---|---|---|---|
| Goat Anti-Rat IgG (Alexa 555) | 2 mg/mL | 1:200 | 10 µg/mL |

20. Wash slides 3 times for 5 minutes with PBS and incubate each chamber slide with 300 µL blocking solution plus CTxB per well at room temperature for 1 hr in a humid chamber. The slides much be protected from light. To properly resuspend antibody, flick and invert 4 times and centrifuge quickly.

| Antibody | Stock | Dilution | Final |
|---|---|---|---|
| Cholera Toxin B (Alexa 488) | 1,000 µg/mL | 1:166 | 6 µg/mL |

21. Prepare the ProLong medium during the last 1 hr antibody incubation by thawing at room temperature for 1 hr with bottle upside down *(stored in -20 °C freezer).*
22. Wash the chamber slides with PBS 3 times for 2 min each.
23. Use slide separator to remove the chamber. Put slides on a slide holder for subsequent washes.
24. Incubate the slides in 70% ethanol once for 30 sec
25. Incubate the slides in 95% ethanol once for 30 sec
26. Incubate the slides in 100% ethanol once for 30 sec
27. Incubate slides in fresh xylene for 30 sec and 2 min. *This means that one would need two fresh xylenes.*
28. Apply a small amount of antifade reagent medium mixture to the coverglass. Cover the slide while it is still wet.
29. Place the slide on a flat surface in the dark to dry overnight at room temperature in the fume hood. Protect from light.
30. **Day 2:** Seal the cover glass to the slide with fingernail polish to prevent shrinkage of mounting medium and subsequent sample distortion.

31. After sealing, let it dry for at least 15 min, then store the slide upright in a slide box at -20°C. Desiccant may be added to the box to ensure that the slide remains dry.
32. Examine sample under fluorescence microscopy. Use Pearson's correlation and Mander's coefficient for co-localization analysis.

APPENDIX F

WESTERN BLOT

**Purpose: To determine the presence of a specific protein (gp130) in a sample using a primary antibody to tag the desired protein and a secondary antibody to visualize the marked protein.**

**Reagents:**

SDS running buffer (Expedeon NXB60500)

Pyronin 5X Sample Buffer

--40% glycerol (Sigma, 119H0206), 25% β-mercaptoethanol (ProPure, 3009B297), 12% SDS (Fisher, BP166-100), 0.31 M Trish Base pH 6.8 (Fisher, cat# BP154-1), 25 mM EDTA (Sigma, ED455-500G), 0.1% Pyronin Y (BioRad, 161-0425)

1X Tris-Glycine and 14% methanol

--To make 2 L, mix 200 mL of 10X Tris-Glycine (Amresco 0783), 280 mL of methanol (Fisher, cat# A433P-4), and 1520 mL of double distilled water

1X PBS-Tween

--Dissolve one bottle of 10X Dulbecco's Phosphate-Buffered Saline (Gibco, cat#21600-069) in one liter of double distilled water and then add 10 g of Tween-20 (Fisher, cat#BP337-500). The Tween-20 should be added directly into the PBS on the scale due to the viscosity of the Tween 20. Dilute this solution down to 1X by adding 100 mL of 10X PBS Tween into 900 mL of double distilled water.

4-20% Tris-Glycine gel (Expedeon NXG42012)

Magic Mark XP Western Standard (invitrogen, LC5620)

Super Signal West Femto Maximum Sensitivity Substrate (Thermo Scientific, 34095)

Immobilon membrane (Millipore, #6MW-2020) (dimensions of 7.4 cm across and 8.5 cm in length)

Filter paper (MidSci, #IPVH00010) (dimensions of 10 cm x 10 cm)

Rabbit anti-mouse gp130 (Santa Cruz sc-656)

Goat anti-rabbit IgG peroxidase conjugated (KPL 074-1506)

**Preparation:**

Make Running Buffer and Transfer buffer and cool before use

- Can be re-used several times

Thaw samples on ice from -80ºC (usually takes about 15 minutes)

Label the top of 0.6 ml eppy tubes

Prepare western blot template sheet.

**Sample Preparation:**

1. The dye used for the sample dilutions is 5X Pyronin. Dilute the dye down to 1X.

a. For example, if you have a total volume of sample + buffer + dye=10, use 2 µl dye (10/5=2)

2. With the aid of the western blot template, dispense the correct amount of dye and double distilled water into the eppy tubes and add the sample last.

3. Flick the ends of the tubes for basic mixing and then quick spin.
4. Boil the samples for 5-10 min depending on the volume of the samples at 98ºC (25 µL volumes are boiled for 10 min). **Do not boil the marker.**
5. Once boiling is complete, flick the ends of the tube for basic mixing and then quick spin.

**Gel unit set up:**
6. While the samples are boiling, take the pre-made gel (4-20%) and carefully rip off and discard the white tape.
7. When clipping the gels or the white sheet to the gel apparatus, the broad side of the clip should be facing you and broad ends face outside on all 4 clips. See figure for visual clarification.

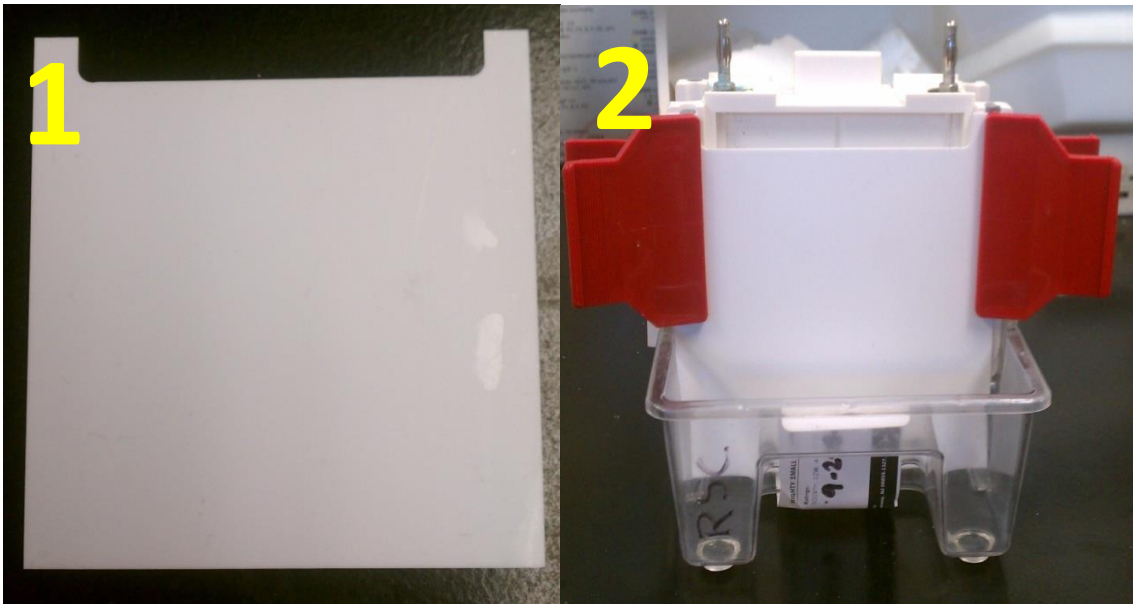


*1. White, metal sheet*
*2. Proper orientation of clips on the gel trough*

8. For attaching one gel, attach the white, metal sheet to adjacent side (make sure that the sheet is pressed all the way to the bottom of the well and against the back of the apparatus). Attach the gel in the same fashion as the white sheet with the gel pressed all the way to the bottom of the trough and against the back of the unit.
9. Pour running buffer in between the gel and the apparatus until a small amount of buffer leaks over the top of the gel.

10. Check to see if there are any leaks by observing the level of the buffer behind the gel.
11. Repeat steps 9 and 10 for the white sheet or the adjacent gel.
12. Once there are no leaks, fill the bottom of the trough on both sides with running buffer up to the top mark. (Cover middle hump)
13. Load the samples into their respective wells. The gel should be loaded in the cold room.
14. Close the unit with the lid and check the leads and make sure black-to-black and red-to-red.
15. In the cold room, run the gel at 125 V until the marker is just above the indention where the white tape was removed (The running of the gel takes about two hours and increase the power, current, and time in the power unit so that these factors do not affect the voltage).
16. Before leaving the cold room, make sure 125 V is reached and check the gel after 10 min to make sure the gel is running properly. If the gel is running properly, the marker and the dye should be running evenly down the gel (run for ~2hrs).

**Gel Transfer:**
17. Take the gel transfer unit in a staining tray and pour transfer buffer into the trough.
18. Take the cassette and lay it open.
19. Put the thick sponge on the black side of the cassette and place the thin sponge on the white side of the cassette.
20. Place a piece of filter paper on each sponge.
21. Pour transfer buffer in the trough to keep the thick sponge and filter paper wet. It is not necessary for the thin sponge to be wet.
22. Take the gel plate out of the running trough and transfer the running buffer into the bottle for reuse.
23. Crack open the plate with a scalpel between the markings on the plate all around by keeping the large side of the gel down.
24. Cut the wells out of the gel and cut just above the bottom to allow separation of the gel from the plastic.
25. Carefully separate the gel from the plate and cut a mark on the gel to keep track of the location of lane one.
26. Place the gel in transfer buffer for 5 min to allow it to equilibrate.
27. Place the gel on the filter paper with lane one on the right side to ensure that the protein will face the membrane.
28. Take the membrane out of the sandwich of protective paper with forceps and wet the membrane in a dish of methanol for about 3 min.
29. Place the membrane on top of the gel and roll out the air bubbles that are between the gel and the membrane (the very bottom of the membrane may be touched when rolling).
30. Place the second filter paper on top of the membrane and roll out the remaining air bubbles.
31. Place the thin sponge on top of the filter paper and carefully close the cassette to prevent the creation of more air bubbles.

32. Place the cassette in the transfer unit with the hinges facing the top and the black side facing the back of the unit.
33. Put a stir bar into the transfer unit.
34. Fill the unit with transfer buffer just enough to cover the hinges of the cassette (ignore the maximum level indicator on the unit).
35. Place the unit in the cold room on the stir plate and set to a speed setting of about 4.
36. Give the unit a final tap and connect black to the back of the unit and red to the front of the unit.
37. Set the current to 400 mA (0.4 A) and allow the transfer to take place for 90 min.

**Blocking:**
Note: For experiments requiring the use of BSA, follow the same protocol as dried milk. Refer to the manufacturer's data sheet to see if BSA or dried milk should be used.

38. At the end of the transfer, make fresh 4% nonfat dry milk/ 1XPBS (0.1%)Tween in a 50 mL tube (30 mL of 1X PBS (0.1%)Tween and 1.2 g of pre-weighted milk powder). Mix gently by inversion.
39. Pour milk into a dish and keep ready to transfer the membrane into it.
40. Open the transfer unit, place membrane into the milk mixture with broad-nosed forceps, and put transfer buffer back into bottle for reuse (make sure side of the membrane with the protein is facing up).
41. Place membrane dish on the shaker (Stovall, Belly Dancer) for 1 hr at room temperature at a speed setting of about 6.

**Primary Antibody:**
42. Prepare a fresh dish of 1.2 g of dry milk and 30 mL of 1X PBS (0.1%)Tween about 5-10 min before blocking is complete. (can do 20 ml if trying to conserve antibody).
43. Pour out milk from previous steps and pour in fresh milk.
44. Now, add the appropriate volume of the primary antibody based on the manufacturer's recommended dilution and the volume added to the dish.
45. Close the lid of the dish and shake at an intensity of 3 in the cold room overnight.

**Washing:**
46. The next day take the membrane and give it a quick wash with 1X PBS (0.1%)Tween. A quick wash is simply pouring out the solution and adding fresh 1X PBS (0.1%)Tween. Keep on the shaker at room temperature for 10 min, and let it shake at a speed setting of about 6. **Do 3 washes!**

**Secondary Antibody:**
47. Make 30 mL of milk/PBS (0.1%)Tween and pour into the dish after the second wash to ensure that it is fresh (1.2 g of dry milk and 30 mL of 1X PBS (0.1%)Tween).
48. After the washing is complete, place the membrane into the fresh milk/1XPBS (0.1%)Tween mixture and add the correct amount of secondary antibody depending on the manufacturer's suggested dilution and the volume of the dish.

49. Set the dish on the shaker for one hour at room temperature with a shaking speed of about 3.
50. Once the shaking is complete, repeat washing with 1X PBS (0.1%)Tween three times (Step 46).

**Developing:**
51. During the washing, turn on the camera and the imager. Then make sure the imager is set to CHEMI.
52. After the 2nd wash is complete, cut an acetate sheet into two halves and remove the black sheet in between.
53. Mix 0.25 mL of chemiluminescent super signal reagent A with 0.25 mL of reagent B in an eppy tube and mix gently by pipetting (Place the tube in the dark until use because this mixture is sensitive to light).
54. Now transfer the membrane with forceps in between the layers of the acetate sheet and squirt the developing solution on the top of the membrane.
55. Slowly close the top layer so that the solution gets evenly distributed on the membrane.
56. Expose to light for five minutes and then transfer the membrane onto a clean acetate sheet. The new acetate sheet does not need to be protected from light.
57. Transfer into the imager and image immediately.

**Imaging:**
58. Select the Quantity One program on the desktop.
59. Select the scanner- click on chemidoc.xrs (there is only one option).
60. Select the option of chemiluminescences and live focus.
61. Focus with a printed sheet and set the iris as you need for brightness. Zoom and focus, as you need for clarification.
62. Freeze. Put the gel in the imager and zoom and freeze again. Close the door.
63. Click on Live Acquire.
64. Starting Exposure time -30 sec.
    Total Exposure time-150 sec.
    Number of exposures- 5
65. Imager takes 5 pictures in 150 sec. (These settings can be adjusted as needed).
66. Turn off machine (2 power buttons) and clean the inside with distilled water and wipe dry. Remember to sign out.

**Expected Results:**
Once the membrane is developed, bands should appear in the size range of the desired protein based on the molecular weight marker. The full marker should also be visualized when developed.

*Storage Conditions of Products and Reagents:*
- Samples should be kept on ice at all times.

- The developing solution should be protected from light until it is ready for use. The developing kit should be stored at 4ºC.
- Running buffer and Transfer buffer should be stored at 4ºC.
- 1X PBS (0.1%)Tween may be stored at room temperature.
- BSA should be stored at 4ºC, but the milk powder can be stored at room temperature.

*Notes:*

- Milk/BSA solution should always be make fresh about 10 min before use.
- Gloves should be worn at all times to preserve the integrity of the membrane and for protection of the hands from harmful reagents.
- For analysis of gp130 protein expression, 4 µg of protein was electrophoresed with a 1° antibody dilution of 1: 2,000 in milk and 2° antibody dilution of 1:10,000 in milk.

APPENDIX G

GP130 DIMERIZATION

**Purpose: To measure the ability of gp130 molecules to form homodimers as a means of assessing function.**

**Reagents:**
Recombinant IL-6 (Biolegend 575704)
Bissulfosuccinimidyl suberate ($BS^3$) (*Thermo Scientific # 21586)*
Glycine (Sigma, G7126)
Homogenization Buffer (See appendix H)
Benzonase (Sigma E1014-25KU)

**Procedure:**
1. Isolate $CD4^+$ T cells according to Appendix A: Isolation of $CD4^+$ T cells Miltenyi bead/column.
    a. *Use 7 million cells per mouse in 1 mL complete RPMI (need two samples- one stimulated with IL-6, one unstimulated).*
2. Stimulate with 100 ng/mL IL-6 for 10 minutes at 37ºC.
3. Spin down at 350g for 5 minutes, aspirate supernatant, wash with 10 mL PBS, spin down, resuspend in 5 mL of 3 mM bis(sulfosuccinimidyl)suberate ($BS^3$) *( MW=572.4)* in ice cold $Ca^{2+}$, $Mg^{2+}$ free PBS for 2 hours at 4°C *(8.60 mg $BS^3$ in 5 mL).*
    a. *This crosslinks proteins that are in contact with each other.*
4. Quench with 10 mL of 250 mM glycine in PBS for 5 min at 4°C.
5. Spin down at 350 x g for 5 minutes, aspirate supernatant, wash with 10 mL PBS, spin down, aspirate supernatant.
6. Add 100 µL of homogenization buffer with 1 µl benzonase to each tube and transfer to a 0.6 mL epi tube.
7. Incubate the total lysate in ice for 30 min.
8. Centrifuge at 16, 000 x g at 4°C for 20 min.
9. Transfer the supernatant (lysate) to clean epi-tube, mix.
10. Aliquot (30 µl) and save aliquots at -80°C for further protein estimation using Coomassie Plus and immunoblotting.

*Notes:*
- Dimers on western blot should be twice the size of the gp130 band (should appear at 260 kDa). Unstimulated cells should not have a dimer band and can be used for control.
- Gel for western blot should be run for approximately 4-5 h at 125 V, and transfer should be overnight at 400 mAmps. Make sure to incubate the gel in transfer buffer for ~15-30 minutes before beginning the transfer.

APPENDIX H

HOMOGENIZATION BUFFER

**Purpose: To homogenize naïve or stimulated CD4+ T cells for western blot analysis.**

| **Component** | **Catalog Number** | **Volume for 10 mL** | **Final Concentration** |
|---|---|---|---|
| 500 mM Tris-HCL (pH 7.2) *(6.1 g/100 mL)* | Fisher Scientific (BP153) | 1 mL | 50 mM |
| 1 M Sucrose (34.23g/100mL) | Sigma (S9378) | 2.5 mL | 250 mM |
| 200 mM EDTA (pH 7.6) 4.162g in 50mL | Sigma (ED4SS) | 0.1 mL | 2 mM |
| 100 mM EGTA (pH 7.5) 0.38 g/10 mL-add NaOH to get it to dissolve and bring pH to 7.5 | Sigma (34596) | 0.1 mL | 1 mM |
| 10% Triton X-100 2 mL up to 20 mL ddH20 | Sigma (T6878) | 1 mL | 1% |
| ddH20 | | 4.7 mL | |

Homogenization Buffer Part A: Can be made ahead and stored at 4°C for a couple days or aliquoted and stored at -20°C.

Part B: Make the day of use

For 1 mL of complete buffer, use 960 µl Part A + ingredients listed below. For 5 mL, add 4,747 µl Part A + ingredients listed below.

| Component | Catalog Number | Volume for 5 mL | Volume for 1 ml | Final Concentration |
|---|---|---|---|---|
| Protease Inhibitor Cocktail | Sigma (P8340) | 0.2 mL | 40 µl | |
| 2 β-mercaptoethanol 14.2 M | Amresco (M131) | 3.5 µl | 0.7 µl | 10 mM |
| Halt Phosphatase Inhibitor (100X) | Thermo Scientific (78428) | 50 µl | 10 µl | 1X |